

# Reconfigurable Intelligent Surface Aided Power Control for Physical-Layer Broadcasting

Huimei Han, Jun Zhao, Wenchao Zhai, Zehui Xiong, Dusit Niyato, *Fellow, IEEE*, Marco Di Renzo, *Fellow, IEEE*, Quoc-Viet Pham, Weidang Lu, and Kwok-Yan Lam, *Senior Member, IEEE*

## Abstract

Reconfigurable intelligent surface (RIS), a recently introduced technology for future wireless communication systems, enhances the spectral and energy efficiency by intelligently adjusting the propagation conditions between a base station (BS) and mobile equipments (MEs). An RIS consists of many low-cost passive reflecting elements to improve the quality of the received signal. In this paper, we study the problem of power control at the BS for the RIS aided physical-layer broadcasting. Our goal is to minimize the transmit power at the BS by jointly designing the transmit beamforming at the BS and the phase shifts of the passive elements at the RIS. Furthermore, to help validate the proposed optimization methods, we derive lower bounds to quantify the average transmit power at the BS as a function of the number of MEs, the number of RIS elements, and the number of antennas at the BS. The simulation results demonstrated that the average transmit power at the BS is close to the lower bound in an RIS aided system, and is significantly lower than the average transmit power in conventional schemes without the RIS.

## Index Terms

Reconfigurable intelligent surface, power control, quality of service, wireless communications.

Huimei Han and Weidang Lu are with Zhejiang University of Technology, Hangzhou, Zhejiang, P.R. China. Jun Zhao, Zehui Xiong, Dusit Niyato and Kwok-Yan Lam are with School of Computer Science and Engineering, Nanyang Technological University, Singapore. Wenchao Zhai is with the China Jiliang University, Hangzhou, Zhejiang, P.R. China. Marco Di Renzo is with Laboratory of Signals and Systems of Paris-Saclay University - CNRS and CentraleSupélec, France. Quoc-Viet Pham is with Research Institute of Computer, Information and Communication, Pusan National University, South Korea. (Emails: {hmhan1215, luweid}@zjut.edu.cn, {junzhao, zxiong002, dniyato, kwokyan.lam}@ntu.edu.sg, zhaiwenchao@cjljlu.edu.cn, marco.direnzo@centralesupelec.fr, vietpq@pusan.ac.kr). Part of the work has been presented in IEEE ICC 2020 [1].

## I. INTRODUCTION

Fifth-generation (5G) communications achieve great improvement in spectral efficiency by utilizing various advanced technologies, such as massive multiple-input multiple-output (MIMO) communications, non-orthogonal multiple access transmission, millimeter (mm)-wave communications, and ultra-dense Heterogeneous Networks. However, the high energy consumption of 5G communications is a critical issue [2]. To improve the spectral efficiency and reduce the energy consumption simultaneously, researchers are exploring new ideas for future wireless systems beyond 5G [3]–[6]. Among solutions, reconfigurable intelligent surface (RIS) can improve coverage capability, spectral efficiency, and quality of the reflected signal by controlling the phase of the incident signal in a passive way. Such good features make RIS a new technology for the 6G communications, and RIS has attracted much attention recently [7]–[13]. An RIS is a planar array consisting of many reflecting and nearly passive units, which intelligently and dynamically adjusts the propagation conditions to improve the communication quality between the base station (BS) and mobile equipments (MEs). Since each RIS unit reflects the signal in a passive way instead of transmitting/receiving signal in an active way, the energy consumption is low. **Furthermore, the RIS has the features of lightweight, low profile, and conformal geometry, making it easy to mount or remove the RIS from objects. If some objects (i.e., UAVs, drones, and buildings) are located between the BS and the RIS, the RIS can be installed on a high rise building or in the air to create a line-of-sight (LoS) link between the BS and the RIS [9], [14]–[16].** Indeed, passive reflecting surfaces have been used in other communication systems, such as radar systems and satellite communication systems, but have received less attention in mobile wireless communication systems up until now.

Broadcast traffic can be used for the BS to broadcast system public control information to MEs. System information broadcasting in the communication system provides information to facilitate MEs to establish wireless connections [17]. Broadcast traffic can also be used for news feed, video-conference, or movie broadcast [18]. To address the problem of power control at the BS for physical layer broadcasting with quality of service (QoS) constraints in RIS aided networks, we propose to employ two alternating optimization algorithms in order to jointly design the transmit beamforming at the BS and the phase shifts of the reflecting units at the RIS. We also present computational complexity analysis of the proposed alternating optimization algorithms. Furthermore, to validate the performance of the optimization algorithms, we derive

two lower bounds for the average transmit power at the BS. Simulation results show that the average transmit power at the BS is close to the lower bounds, and is much lower than the average transmit power of communication systems without the RIS. Specifically, the main features and contributions of this paper can be summarized as follows.

- We formulate a BS power control optimization problem for physical layer broadcasting under QoS constraints in the RIS aided network. We propose two alternating optimization algorithms for solving it. Specifically, we propose an alternating optimization algorithm based on semidefinite relaxation (SDR) technique to obtain the minimum transmit power. To reduce computational complexity and improve the performance, we also propose an alternating optimization algorithm based on successive convex approximation (SCA) method.
- We introduce two lower bounds providing information on the average transmit power at the BS as a function of the number of MEs, the number of RIS units, and the number of antennas at the BS, considering a full-rank LoS channel between the BS and the RIS. These lower bounds are employed to analyze the effectiveness of the proposed optimization algorithms. In particular, we propose an analytical and a semi-analytical lower bounds. The first bound is easier to compute but the second one is tighter. Simulation results demonstrate that the average transmit power at the BS is close to the semi-analytical lower bound.
- With the aid of numerical simulations, we compare the performance of the proposed algorithms against a two-stage algorithm and conventional schemes without RISs.

As opposed to the conference version in [1], we make the following extensions.

- In contrast to the BS-to-RIS rank-one LoS channel scenario in [1], we consider a full rank LoS channel to benefit from the RIS in the broadcasting multi-MEs setting [9].
- In [1], we briefly introduced an alternating optimization algorithm based on the SDR technique to obtain the minimum transmit power. In this paper, we not only discuss the alternating optimization algorithm based on the SDR technique in detail, but also propose an alternating optimization algorithm based on the SCA method to reduce the computational complexity and improve the performance, by utilizing the characteristic of no multi-user interference in the broadcast scenario.
- In [1], we introduced only an analytical lower bound for the average transmit power with the RIS. In this paper, for benchmarking purposes, we also derive analytical lower bounds for the transmit power without the RIS and with random phase shifts at the RIS. Furthermore,

to get a tighter lower bound, we introduce a semi-analytical lower bound.

**Organization.** The remainder of this paper is organized as follows. In Section II, we describe existing research works related to the present paper. Section III introduces the system model and formulates the power control optimization problem for physical-layer broadcasting under QoS constraints. In Section IV, we introduce the proposed algorithms to solve the problem. Two lower bounds for the minimum transmit power are derived in Section V. Sections VI and VII provide numerical results and conclude this paper, respectively.

**Notation.** The notations utilized throughout this paper are described in Table I.

TABLE I: notations.

Notations	Description
Italic letters	Scalars
Boldface lower-case	Vectors
Boldface upper-case letters	Matrices
$(\cdot)^T$ and $(\cdot)^H$	The transpose and conjugate transpose of a matrix
$D_{i,q}$	The element in the $i^{th}$ row and $q^{th}$ column of a matrix $D$
$x_i$	The $i^{th}$ element of a vector $x$
$\mathbb{C}$	The set of all complex numbers
$\mathcal{CN}(\mu, \sigma^2)$	A circularly-symmetric complex Gaussian distribution with mean $\mu$ and variance $\sigma^2$
$\ \cdot\ $	The Euclidean norm of a vector
$ \cdot $	The cardinality of a set
$\text{diag}(x)$	A diagonal matrix with the element in the $i^{th}$ row and $i^{th}$ column being the $i^{th}$ element in $x$
$\arg(x)$	A phase vector
$\mathbb{E}(\cdot)$	The expectation operator
$\text{Var}(\cdot)$	The variance operator
$M^{-1}$ and $M \succeq 0$	The inverse of a square matrix $M$ and positive semi-definiteness
$I$	The identity matrix
$\Re(c)$ , $\Im(c)$ and $\varphi_c$	The real part, imaginary part and angle of a complex number $c$

## II. RELATED WORKS

In this section, we discuss the existing research works that are related to the present paper.

**Power control in RIS aided communications.** Power control has been studied in several recent papers on RIS aided communications. Wu and Zhang minimized the transmit power at the BS by optimizing the transmit beamforming at the BS and the phase shifts of the RIS, subject to signal-to-interference-plus-noise ratio (SINR) constraints at MEs [7]. They extended the study in [7] to account for discrete phase shifts in [8] and [19]. Zhou *et al.* extended [7] to consider power control in RIS aided communications under imperfect channel state information (CSI) [20]. The problem of power control when an RIS is used to achieve secure communications was investigated in [21], [22]. Recent studies [23], [24] tackled transmit power minimization in RIS aided networks with non-orthogonal multiple-access (NOMA). Different from [1], [7], [8],

[19], [25] that addressed only information transfer, Wu and Zhang considered power control for simultaneous wireless information and power transfer in RIS aided systems [26].

**Broadcast/multicast traffic in RIS aided communications.** The above mentioned papers consider the unicast setting, where the BS sends different data to different MEs. We are only aware of a few recent studies on broadcast/multicast traffic in the context of RIS aided communications. The multicast setting categorizes MEs into a number of groups, where MEs in the same group receive the same data from the BS. Zhou *et al.* maximized the sum rate of groups in the multicast setting [27]. In the broadcast case, Du *et al.* maximized the information rate under transmit power constraints, where the system model only involves the indirect channels between the BS and MEs, and analyzed the asymptotic growth of the capacity [28]. In addition, Nadeem *et al.* showed that RISs achieve better performance when the BS-RIS LoS channel is of full rank for a multi-MEs setting [9]. Both [27] and [28] do not consider power control and do not assume a full-rank LoS channel model between the BS and the RIS, as addressed in this paper. In addition, an earlier draft [25] (not submitted) of our paper summarized problems related to power control under QoS in the unicast, multicast, and broadcast settings, but only SDR-based algorithms were briefly presented without any analysis and simulation validation.

**Power control in traditional communication systems without RIS.** In the absence of RIS, downlink power control under QoS for the broadcast setting was studied in the seminal work of Sidiropoulos *et al.* [29]. The problem was also shown to be NP-hard [29]. Karipidis *et al.* extended [29] to the multicast scenario [30]. Power control for multicast traffic in NOMA systems was addressed in [31].

**Comparing RIS with other technologies.** The main advantage of RISs over existing technologies (such as massive MIMO communication [32], mmWave communication [33], amplify-and-forward relaying [34]) is that the RIS comprises only passive elements, achieves low hardware cost, low energy consumption, and intelligently adjusts the wireless environment [7], [35].

**RIS implementations.** To validate the feasibility RIS aided systems, Xin *et al.* implemented a reflecting array for IEEE 802.11 ad for application to mmWave communications [36]. Tang *et al.* experimentally verified channel models for different cases in RIS aided communication systems [37]. Examples of RIS aided communication prototypes were described in [38], [39].

**Other studies of RIS.** In addition to the papers discussed above, there are many other RIS studies that address various optimization problems and emerging applications. Some machine learning based methods were proposed for the phase shifts optimization. Huang *et al.* proposed a

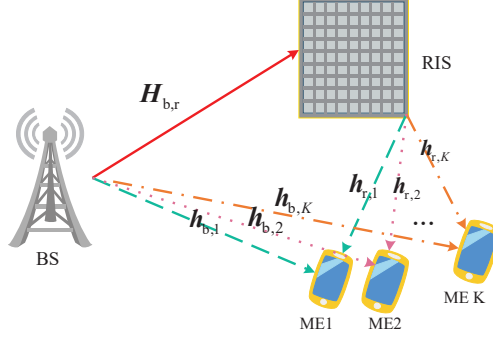


Fig. 1: An RIS aided communication system consisting of a base station (BS), multiple mobile equipments (MEs), and an RIS comprising many RIS units.

deep learning (DL) method of reconfiguring RIS online for the complex indoor environment [4]. Yang *et al.* proposed a win or learn fast policy hill-climbing learning approach to jointly optimize the anti-jamming power allocation and reflecting beamforming [40]. We refer interested readers to a recent surveys [3], [41] and the references therein.

### III. SYSTEM MODEL AND PROBLEM DEFINITION

#### A. System model

We consider an RIS aided multi-input single-output (MISO) communication system in a broadcast setting, where there is a BS with  $M$  antennas and an RIS with  $N$  reflecting units, and  $K$  single-antenna MEs, as shown in Fig. 1. The BS uses linear transmit precoding (i.e., beamforming) that is denoted by the vector  $\mathbf{w} \in \mathbb{C}^{M \times 1}$ . So, the transmitted signal at the BS is  $\mathbf{x} = \mathbf{w}s$ , where  $s$  is the broadcasted data signal. The signal  $\mathbf{x}$  reaches each ME via both indirect and direct channels, and the received signal at each ME is the sum of the signals from these two channels. More specifically, for the indirect channel, the transmitted signal  $\mathbf{x}$  travels from the BS to the RIS, it is then reflected by the RIS, and finally travels from the RIS to these  $K$  MEs. For the direct channel, the transmitted signal  $\mathbf{x}$  travels from the BS to these  $K$  MEs directly.

Let  $\Phi = \text{diag}(\beta_1 e^{j\theta_1}, \dots, \beta_n e^{j\theta_n}, \dots, \beta_N e^{j\theta_N})$  denote the reflection coefficients matrix at the RIS, where  $\beta_n$  and  $\theta_n$  denote the amplitude and phase shift, respectively, and  $j$  is the unit imaginary number. Similar to other recent studies [7]–[9], we assume that the RIS changes only the phase of the reflected signal, i.e.,  $\theta_n \in [0, 2\pi)$  and  $\beta_n = 1^1$ . Let  $\mathbf{H}_{b,r} \in \mathbb{C}^{N \times M}$ ,

<sup>1</sup>Since each element of the RIS is usually designed to maximize the signal reflection, we set the amplitudes of all RIS elements to 1 for simplicity in our papers [7]. When the reflection amplitude depends on the phase shift, the reflection design proposed in this paper is no longer optimal in general and will cause performance degradation [42], and we will do some research on the coupling of reflection amplitude and phase shift in the future.

$\mathbf{h}_{r,i}^H \in \mathbb{C}^{1 \times N}$ , and  $\mathbf{h}_{b,i}^H \in \mathbb{C}^{1 \times M}$  be the BS-RIS channel, RIS- $i^{\text{th}}$  ME channel, and BS- $i^{\text{th}}$  ME channel, respectively (the subscripts b, r, and  $i$  represent the BS, the RIS, and the  $i^{\text{th}}$  ME, respectively). Then, the received signal at ME  $i$  is given by

$$y_i = (\mathbf{h}_{r,i}^H \Phi \mathbf{H}_{b,r} + \mathbf{h}_{b,i}^H) \mathbf{w} s + n_i, \quad i = 1, \dots, K, \quad (1)$$

where  $n_i \sim \mathcal{CN}(0, \sigma_i^2)$  denotes the additive white Gaussian noise at the  $i^{\text{th}}$  ME.

We assume that the broadcasted data signal  $s$  is normalized to have unit power. Then, the signal-to-noise ratio (SNR) at the  $i^{\text{th}}$  ME can be written as

$$\text{SNR}_i = \frac{|\mathbf{h}_i^H(\Phi) \mathbf{w}|^2}{\sigma_i^2}, \quad i = 1, \dots, K, \quad (2)$$

where  $\mathbf{h}_i^H(\Phi) = \mathbf{h}_{r,i}^H \Phi \mathbf{H}_{b,r} + \mathbf{h}_{b,i}^H$  denotes the overall downlink channel from the BS to ME  $i$ .

### B. Problem definition

Our research problem on power control is to minimize the transmitted power at the BS for broadcasting under QoS constraints. Note that the transmitted power at the BS is  $\|\mathbf{w}\|^2$ , and the QoS of the  $i^{\text{th}}$  ME can be characterized by its SNR, which is required to be at least  $\gamma_i$ . Then, the optimization problem can be formulated as follows.

$$\text{(P1): } \min_{\mathbf{w}, \Phi} \|\mathbf{w}\|^2 \quad (3a)$$

$$\text{s.t. } \frac{|\mathbf{h}_i^H(\Phi) \mathbf{w}|^2}{\sigma_i^2} \geq \gamma_i, \quad i = 1, \dots, K, \quad (3b)$$

$$0 \leq \theta_n < 2\pi, \quad n = 1, \dots, N. \quad (3c)$$

Let us define the normalized channel vector  $\hat{\mathbf{h}}_i(\Phi) := \frac{\mathbf{h}_i(\Phi)}{\sigma_i \sqrt{\gamma_i}}$  [18]. Then, the constraint (3b) can be transformed as  $|\hat{\mathbf{h}}_i(\Phi) \mathbf{w}|^2 \geq 1$ . This indicates that, though  $\gamma_i$  is different for different MEs,  $\gamma_i$  can be coupled into the channel vector of each ME, thereby all MEs having the same threshold. In our paper, similar to other recent studies [7], [8], [43], we consider that all MEs have the same threshold and noise variance for simplicity (i.e.,  $\gamma_i = \gamma$ ,  $\sigma_i^2 = \sigma^2$ ,  $\forall i = 1, \dots, K$ ).

## IV. ALTERNATING OPTIMIZATION ALGORITHMS

Problem (P1) is NP-hard since even the setup without RIS is NP-hard according to [29]. To solve Problem (P1), we utilize the alternating optimization to perform the following operations iteratively: optimize  $\mathbf{w}$  given  $\Phi$ , and optimize  $\Phi$  given  $\mathbf{w}$ . Under this framework, we propose two algorithms based on SDR and SCA, respectively.

### A. Alternating optimization algorithm based on SDR

---

**Algorithm 1** Alternating optimization based on SDR to find  $\mathbf{w}$  and  $\Phi$  for Problem (P1).

---

- 1: Initialize  $\Phi$  as  $\Phi^{(0)} := \text{diag}(e^{j\theta_1^{(0)}}, \dots, e^{j\theta_N^{(0)}})$ , where  $\theta_n^{(0)}$  ( $n = 1, 2, \dots, N$ ) is chosen uniformly at random from  $[0, 2\pi)$ ;
  - 2: Initialize the iteration number  $q \leftarrow 1$ ;
  - 3: **while** 1 **do**  
     {*Comment: Optimizing  $\mathbf{w}$  given  $\Phi$ :*}
  - 4:   Given  $\Phi$  as  $\Phi^{(q-1)}$ , solve Problem (P3) to obtain  $\mathbf{w}^{(q)}$ ;
  - 5:   Compute the object function value  $P_t^{(q)} \leftarrow \|\mathbf{w}^{(q)}\|^2$ ;
  - 6:   **if**  $1 - \frac{P_t^{(q)}}{P_t^{(q-1)}} \leq \varepsilon$  **then**
  - 7:     **break**; {*Comment:  $\varepsilon$  controls the number of executed iterations before termination. The algorithm terminates if the relative difference between the transmit power obtained during the  $q^{\text{th}}$  iteration and the  $(q-1)^{\text{th}}$  iteration is no greater than  $\varepsilon$ .*}
  - 8:   **end if**  
     {*Comment: Finding  $\Phi$  given  $\mathbf{w}$ :*}
  - 9:   Given  $\mathbf{w}$  as  $\mathbf{w}^{(q)}$ , solve Problem (P7) to obtain  $\Phi^{(q)}$ ;
  - 10:   **if** Problem (P7) is infeasible **then**
  - 11:     **break**;
  - 12:   **end if**
  - 13: **end while**
- 

The SDR-based alternating optimization is shown in Algorithm 1. The details of the  $q^{\text{th}}$  iteration are described as follows.

**Optimizing  $\mathbf{w}$  given  $\Phi^{(q-1)}$ .** Given  $\Phi^{(q-1)}$ , Problem (P1) reduces to a conventional power control problem under QoS in the downlink broadcast channel in the absence of the RIS:

$$(P2): \min_{\mathbf{w}} \|\mathbf{w}\|^2 \tag{4a}$$

$$\text{s.t. } \frac{|\mathbf{h}_i^H(\Phi^{(q-1)})\mathbf{w}|^2}{\sigma^2} \geq \gamma, \quad i = 1, \dots, K. \tag{4b}$$

Problem (P2) is non-convex because of the non-convex constraints (4b). Define  $\mathbf{X} := \mathbf{w}\mathbf{w}^H$  and  $\mathbf{H}_i(\Phi^{(q-1)}) := \mathbf{h}_i(\Phi^{(q-1)})\mathbf{h}_i(\Phi^{(q-1)})^H$ . Then, Problem (P2) can be rewritten as [44]

$$(P3): \min_{\mathbf{X}} \text{trace}(\mathbf{X}) \tag{5a}$$

$$\text{s.t. } \text{trace}(\mathbf{X}\mathbf{H}_i(\Phi^{q-1})) \geq \gamma\sigma^2, \quad i = 1, \dots, K, \tag{5b}$$

$$\mathbf{X} \succeq 0, \quad \text{rank}(\mathbf{X}) = 1. \tag{5c}$$

We employ SDR to drop the non-convex rank-one constraint in (5c). Therefore, Problem (P3) reduces to a semi-definite program (SDP), and we can utilize conventional optimization software (e.g., CVX [45]) to solve it. Generally, SDR may not produce a rank-one solution to Problem (P3). Thus, once  $\mathbf{X}$  is available, the Gaussian randomization method [46] is usually



applied to obtain rank-one solutions to Problem (P3). Specifically, by utilizing the eigenvalue decomposition,  $\mathbf{X}$  can be rewritten as  $\mathbf{X} = \mathbf{U}\mathbf{\Lambda}\mathbf{U}^H$  where  $\mathbf{U}$  and  $\mathbf{\Lambda}$  are a unitary matrix and a diagonal matrix, respectively. Then, a suboptimal solution to Problem (P3) is given by  $\mathbf{X}_s = \mathbf{U}\mathbf{\Lambda}^{1/2}\mathbf{r}$ , where  $\mathbf{r}$  is a random vector whose distribution is  $\mathcal{CN}(0, \mathbf{I}_M)$  with  $\mathbf{I}_M$  being the identity matrix. When utilizing the Gaussian randomization, we can obtain multiple candidate solutions to Problem (P3), and we regard  $\mathbf{w}^{(q-1)}$  as a candidate solution to Problem (P3) to ensure the convergence of the proposed SDR-based algorithm as shown in Proposition 1. Then, we select the candidate solution with the minimum transmit power at the BS as the value of  $\mathbf{w}$  during the  $q^{\text{th}}$  iteration, denoted by  $\mathbf{w}^{(q)}$ .

**Finding  $\Phi$  given  $\mathbf{w}^{(q)}$ .** Given  $\mathbf{w}^{(q)}$ , Problem (P1) boils down to the following feasibility check problem of finding  $\Phi$ :

$$(P4) : \text{Find } \Phi \tag{6a}$$

$$\text{s.t. } \frac{|\mathbf{h}_i^H(\Phi)\mathbf{w}^{(q)}|^2}{\sigma^2} \geq \gamma, \quad i = 1, \dots, K, \tag{6b}$$

$$0 \leq \theta_n < 2\pi, \quad n = 1, \dots, N. \tag{6c}$$

Define  $\phi = [e^{j\theta_1}, \dots, e^{j\theta_N}]^H$ ,  $\mathbf{a}_i = \text{diag}(\mathbf{h}_{r,i}^H)\mathbf{H}_{b,r}\mathbf{w}^{(q)}$ , and  $b_i = \mathbf{h}_{b,i}^H\mathbf{w}^{(q)}$ . Then, Problem (P4) can be rewritten as

$$(P5) : \text{Find } \phi \tag{7a}$$

$$\text{s.t. } \begin{bmatrix} \phi^H, & 1 \end{bmatrix} \mathbf{A}_i \begin{bmatrix} \phi \\ 1 \end{bmatrix} + b_i b_i^H \geq \gamma \sigma^2, \quad i = 1, \dots, K, \tag{7b}$$

$$|\phi_n| = 1, \quad n = 1, \dots, N, \tag{7c}$$

where  $\mathbf{A}_i = \begin{bmatrix} \mathbf{a}_i \mathbf{a}_i^H & \mathbf{a}_i b_i^H \\ b_i \mathbf{a}_i^H & 0 \end{bmatrix}$ ,  $i = 1, \dots, K$ . Note that, since the constraints in (7c) are non-convex, Problem (P5) is a non-convex optimization problem. Let us introduce an auxiliary variable  $t$  satisfying  $|t| = 1$ , and define  $\mathbf{v} := t \begin{bmatrix} \phi \\ 1 \end{bmatrix} = \begin{bmatrix} \phi t \\ t \end{bmatrix}$ ,  $\mathbf{V} := \mathbf{v} \mathbf{v}^H$ . Problem (P5) can then be transformed into the following problem

$$(P6) : \text{Find } \mathbf{V} \tag{8a}$$

$$\text{s.t. } \text{trace}(\mathbf{A}_i \mathbf{V}) + b_i b_i^H \geq \gamma \sigma^2, \quad i = 1, \dots, K, \tag{8b}$$

$$\mathbf{V} \succeq 0, \quad \text{rank}(\mathbf{V}) = 1, \quad \mathbf{V}_{n,n} = 1, \quad n = 1, \dots, N + 1. \tag{8c}$$

Similar to Problem (P3), SDR is utilized to drop the non-convex rank-one constraint for  $\mathbf{V}$ . To accelerate the optimization process, the variables  $\alpha_i$  ( $i = 1, \dots, K$ ) are further introduced [7]:

$$(P7) : \max_{\mathbf{V}, \alpha} \sum_{i=1}^K \alpha_i \quad (9a)$$

$$\text{s.t.} \quad \text{trace}(\mathbf{A}_i \mathbf{V}) + b_i b_i^H \geq \alpha_i + \gamma \sigma^2, \quad i = 1, \dots, K, \quad (9b)$$

$$\mathbf{V} \succeq 0, \mathbf{V}_{n,n} = 1, \alpha_i \geq 0, \quad n = 1, \dots, N+1, \quad i = 1, \dots, K. \quad (9c)$$

Similar to Problem (P3), we can utilize the CVX software [45] to solve Problem (P7). Generally, the SDR may not produce the rank-one solution to Problem (P7). Thus, once  $\mathbf{V}$  is available, the Gaussian randomization method [46] is again applied to obtain many candidate rank-one solutions to Problem (P7), which are denoted by  $[\Phi_1^{(q)}, \dots, \Phi_c^{(q)}]$  where  $c$  is the number of candidate solutions. In particular, to select one from these  $c$  candidate solutions as the value of  $\Phi$  during the  $q^{\text{th}}$  iteration, which is denoted by  $\Phi^{(q)}$ , we use the following procedure.

Let  $P_t = \|\mathbf{w}\|^2$  denote the transmit power. Given  $\Phi$ , Problem (P2) is rewritten as

$$\begin{aligned} & \min_{\bar{\mathbf{w}}, P_t} P_t \\ & \text{s.t.} \quad \frac{P_t |\mathbf{h}_i^H(\Phi) \bar{\mathbf{w}}|^2}{\sigma^2} \geq \gamma, \quad \forall i \in \{1, 2, \dots, K\}. \end{aligned} \quad (10)$$

We define  $f := \min(|\mathbf{h}_1^H(\Phi) \bar{\mathbf{w}}|^2, \dots, |\mathbf{h}_K^H(\Phi) \bar{\mathbf{w}}|^2)$ , where  $\bar{\mathbf{w}} = \frac{\mathbf{w}}{\|\mathbf{w}\|}$  denotes the transmit beamforming direction at the BS. By direct inspection, the minimum value of  $P_t$  is

$$P_t = \frac{\gamma \sigma^2}{\min(|\mathbf{h}_1^H(\Phi) \bar{\mathbf{w}}|^2, \dots, |\mathbf{h}_K^H(\Phi) \bar{\mathbf{w}}|^2)} = \frac{\gamma \sigma^2}{f}. \quad (11)$$

We can see from (11) that, given  $\bar{\mathbf{w}}$ , the larger the value of  $f$ , the smaller the value of  $P_t$ . Therefore, we select the candidate solution of  $\Phi$  that maximizes  $f$  as  $\Phi^{(q)}$ . The maximum value of  $f$  is denoted by  $f_{\circ\Phi}^{(q)}$  (the subscript ‘‘o’’ denotes optimized). In order to ensure that the objective value in Problem (P2) is non-increasing over the iterations (as detailed in Proposition 1),  $f_{\circ\Phi}^{(q)}$  needs to satisfy the condition  $f_{\circ\Phi}^{(q)} \geq f_{\circ\mathbf{w}}^{(q)}$ , where  $f_{\circ\mathbf{w}}^{(q)}$  is the value of  $f$  after optimizing  $\mathbf{w}$  given  $\Phi^{(q-1)}$ .  $f_{\circ\mathbf{w}}^{(q)}$  is obtained by replacing  $\Phi$  and  $\bar{\mathbf{w}}$  in (11) with  $\Phi^{(q-1)}$  and  $\bar{\mathbf{w}}^{(q)} = \frac{\mathbf{w}^{(q)}}{\|\mathbf{w}^{(q)}\|}$ , respectively. If  $f_{\circ\Phi}^{(q)} < f_{\circ\mathbf{w}}^{(q)}$ , the iteration process ends.

**Proposition 1.** *The proposed SDR-based alternating algorithm is convergent.*

**Proof:** The convergence of the proposed SDR-based alternating algorithm is guaranteed by the following two facts. First, the objective value in Problem (P2) is non-increasing over iterations.

More specifically, if the value of  $f$  after optimizing  $\mathbf{w}$  given  $\Phi$  is non-decreasing over the iterations, then  $P_t$  is non-increasing over the iterations. That is, if  $f_{\text{ow}}^{(q+1)} \geq f_{\text{ow}}^{(q)}$ , we have  $P_t^{(q+1)} \leq P_t^{(q)}$ . The rule of selecting  $\Phi^{(q)}$  ensures  $f_{\text{o}\Phi}^{(q)} \geq f_{\text{ow}}^{(q)}$ , which also makes  $\mathbf{w}^{(q)}$  a solution to Problem (P3) in the  $(q+1)^{\text{th}}$  iteration. We regard  $\mathbf{w}^{(q)}$  as one of the candidate solutions to Problem (P3), and select the candidate solution with the minimum transmit power at the BS as  $\mathbf{w}^{(q+1)}$  to ensure that  $\mathbf{w}^{(q+1)}$  does not decrease the transmit power. Then, we have  $f_{\text{ow}}^{(q+1)} \geq f_{\text{o}\Phi}^{(q)}$  based on (11). Hence, we have  $f_{\text{ow}}^{(q+1)} \geq f_{\text{o}\Phi}^{(q)} \geq f_{\text{ow}}^{(q)}$  and  $P_t^{(q+1)} \leq P_t^{(q)}$ , which means that  $P_t$  is non-increasing over the iterations, i.e., the objective value in Problem (P2) is non-increasing over the iterations. Second, the optimal value is bounded from below due to the SNR constraints for Problem (P2). Therefore, the proposed SDR-based alternating algorithm is convergent.  $\square$

### B. Alternating optimization algorithm based on SCA

Problem (P1) is NP-hard, and we have utilized the SDR-based alternating optimization algorithm to solve this problem in Section IV-A. However, SDR causes performance loss, and the complexity of solving Problems (P2) and (P4) is high (a detailed discussion is available in Section IV-C). To reduce the computational complexity and improve the performance, we propose an alternating optimization algorithm based on SCA to solve Problem (P1), which is shown in Algorithm 2. Specifically, we employ the SCA method to solve Problem (P2) and to reduce the computational complexity, and introduce a variable  $g$  to solve Problem (P4) in order to maximize the value of  $\min(|\mathbf{h}_1^H(\Phi)\mathbf{w}|^2, \dots, |\mathbf{h}_K^H(\Phi)\mathbf{w}|^2)$  when optimizing  $\Phi$  given  $\mathbf{w}$ .

**Optimizing  $\mathbf{w}$  given  $\Phi^{(q-1)}$ .** Given  $\Phi^{(q-1)}$  obtained during the  $(q-1)^{\text{th}}$  iteration, Problem (P1) becomes the conventional power control Problem (P2). Problem (P2) is non-convex because of the non-convex constraints in Inequalities (4b), and Section IV-A utilizes SDR to solve Problem (P2). To reduce the computation complexity, we utilize the SCA-based method in [47] to solve Problem (P2). Specifically, Problem (P2) is equivalent to

$$(P8): \quad \min_{\mathbf{w}, \{x_i, y_i, \forall i\}} \quad \|\mathbf{w}\|^2 \quad (12a)$$

$$\text{s.t.} \quad x_i^2 + y_i^2 \geq \gamma\sigma^2, \quad i = 1, \dots, K, \quad (12b)$$

$$x_i = \Re(\mathbf{h}_i^H(\Phi^{(j-1)})\mathbf{w}), y_i = \Im(\mathbf{h}_i^H(\Phi^{(j-1)})\mathbf{w}), \quad i = 1, \dots, K, \quad (12c)$$

where the set of constraints in Inequalities (12b) are still non-convex. To tackle the non-convexity, we employ the SCA method where  $\mathbf{w}$  is obtained iteratively. Specifically, let us define  $\mathbf{r}_i :=$

---

**Algorithm 2** Alternating optimization based on SCA to find  $\mathbf{w}$  and  $\Phi$  for Problem (P1).

---

- 1: Initialize  $\Phi$  as  $\Phi^{(0)} := \text{diag}(e^{j\theta_1^{(0)}}, \dots, e^{j\theta_N^{(0)}})$ , where  $\theta_n^{(0)}$  ( $n = 1, 2, \dots, N$ ) is chosen uniformly at random from  $[0, 2\pi)$ ;
  - 2: Initialize the iteration number  $q \leftarrow 1$ ;
  - 3: **while** 1 **do**  
    {*Comment: Optimizing  $\mathbf{w}$  given  $\Phi$ :*}
  - 4:   Given  $\Phi$  as  $\Phi^{(q-1)}$ , solve Problem (P8) to obtain  $\mathbf{w}^{(q)}$ ;
  - 5:   Compute the object function value  $P_t^{(q)} \leftarrow \|\mathbf{w}^{(q)}\|^2$ ;
  - 6:   **if**  $1 - \frac{P_t^{(q)}}{P_t^{(q-1)}} \leq \varepsilon$  **then**
  - 7:     **break**; {*Comment:  $\varepsilon$  controls the number of executed iterations before termination. The algorithm terminates if the relative difference between the transmit power obtained during the  $q^{\text{th}}$  iteration and the  $(q-1)^{\text{th}}$  iteration is no greater than  $\varepsilon$ .*}
  - 8:   **end if**  
    {*Comment: Finding  $\Phi$  given  $\mathbf{w}$ :*}
  - 9:   Given  $\mathbf{w}$  as  $\mathbf{w}^{(q)}$ , solve Problem (P9) to obtain  $\Phi^{(q)}$ ;
  - 10:   **if** Problem (P9) is infeasible **then**
  - 11:     **break**;
  - 12:   **end if**
  - 13: **end while**
- 

$(x_i, y_i)^T$ . Based on the SCA method [47], during the  $d^{\text{th}}$  iteration, the left-hand side of the constraints in Inequalities (12b) can be written as

$$x_i^2 + y_i^2 = \mathbf{r}_i^T \mathbf{r}_i \geq \left\| \mathbf{p}_i^{(d)} \right\|^2 + 2 \sum_{b=1}^2 p_{i,b}^{(d)} (r_{i,b} - p_{i,b}^{(d)}), \quad i = 1, \dots, K, \quad (13)$$

where  $\mathbf{p}_i$  is a parameter vector which is updated as  $\mathbf{p}_i^{(d+1)} = \mathbf{r}_i^{(d)}$  during the  $(d+1)^{\text{th}}$  iteration, and  $p_{i,b}$  and  $r_{i,b}$  stand for the  $b^{\text{th}}$  component of vector  $\mathbf{p}_i$  and  $\mathbf{r}_i$ , respectively. During each step of the iterative procedure, the convexity of  $\mathbf{r}_i^T \mathbf{r}_i$  and the first order Taylor approximation ensures that the right-hand side bounds the left-hand side from below in (13) [47]. During the  $d^{\text{th}}$  iteration, Problem (P8) can be written as [47]

$$\text{(P8')} : \quad \min_{\mathbf{w}, \{x_i, y_i, \forall i\}} \quad \|\mathbf{w}\|^2 \quad (14a)$$

$$\text{s.t.} \quad \left\| \mathbf{p}_i^{(d)} \right\|^2 + 2 \sum_{b=1}^2 p_{i,b}^{(d)} (r_{i,b} - p_{i,b}^{(d)}) \geq \gamma \sigma^2, \quad i = 1, \dots, K, \quad (14b)$$

$$x_i = \Re(\mathbf{h}_i^H(\Phi^{(j-1)})\mathbf{w}), y_i = \Im(\mathbf{h}_i^H(\Phi^{(j-1)})\mathbf{w}), \quad i = 1, \dots, K, \quad (14c)$$

where  $\mathbf{p}_i$  is initialized with a value that is in the feasible set of Problem (P8'). The iterative procedure for solving Problem (P8) is outlined in Algorithm 3.

**Finding  $\Phi$  given  $\mathbf{w}^{(a)}$ .** As shown in Section IV-A, by introducing an auxiliary variable  $t$ , Problem (P4) is converted into Problem (P6). Furthermore, (11) shows that minimizing the transmit power is equivalent to maximizing  $\min(|\mathbf{h}_1^H(\Phi)\overline{\mathbf{w}}|^2, \dots, |\mathbf{h}_K^H(\Phi)\overline{\mathbf{w}}|^2)$ . Hence, we introduce

---

**Algorithm 3** SCA method to find  $\mathbf{w}$  for (P8).

---

```

1: Initialize  $\mathbf{p}_i$  as  $\mathbf{p}_i^{(0)}$ : Randomly generate  $\mathbf{p}_i^{(0)}$  that belongs to the feasible set of Problem (P8');
2: Initialize the iteration number  $d \leftarrow 1$ ;
3: while 1 do
4:   Solve (P8') by utilizing convex optimization software (e.g., CVX [45]);
5:   Set  $\mathbf{p}_i^{(d+1)} = \mathbf{r}_i^{(d)}$  and update  $d = d + 1$ ;
6:   if Convergent or reach the required number of iteration then
7:     break;
8:   end if
9: end while

```

---

an auxiliary variable  $g$  to maximize  $\min(|\mathbf{h}_1^H(\Phi)\mathbf{w}|^2, \dots, |\mathbf{h}_i^H(\Phi)\mathbf{w}|^2, \dots, |\mathbf{h}_K^H(\Phi)\mathbf{w}|^2)$  where  $|\mathbf{h}_i^H(\Phi)\mathbf{w}|^2 = \text{trace}(\mathbf{A}_i\mathbf{V}) + b_i b_i^H$ , which is equivalent to maximizing  $\min(|\mathbf{h}_1^H(\Phi)\bar{\mathbf{w}}|^2, \dots, |\mathbf{h}_K^H(\Phi)\bar{\mathbf{w}}|^2)$ , because  $|\mathbf{h}_i^H(\Phi)\mathbf{w}|^2 = P_t |\mathbf{h}_i^H(\Phi)\bar{\mathbf{w}}|^2$  and  $P_t$  is constant during this step. Thus, Problem (P6) can be further transformed to

$$(P9) : \max_{\mathbf{V}, g} g \quad (15a)$$

$$\text{s.t.} \quad \text{trace}(\mathbf{A}_i\mathbf{V}) + b_i b_i^H \geq g + \gamma\sigma^2, \quad i = 1, \dots, K, \quad (15b)$$

$$\mathbf{V} \succeq 0, \quad g \geq 0, \quad \mathbf{V}_{n,n} = 1, \quad n = 1, \dots, N + 1. \quad (15c)$$

We can utilize the CVX software [45] to solve Problem (P9). Generally, the SDR may not produce a rank-one solution to Problem (P9). Thus, once  $\mathbf{V}$  is available, we use again the Gaussian randomization [46] method to obtain multiple candidate rank-one solutions to Problem (P9), and we select the one with the maximum value of  $\min(|\mathbf{h}_1^H(\Phi)\mathbf{w}|^2, \dots, |\mathbf{h}_K^H(\Phi)\mathbf{w}|^2)$  as the value of  $\Phi$  during the  $q^{\text{th}}$  iteration, which is denoted by  $\Phi^{(q)}$ .

**Proposition 2.** *The proposed SCA-based alternating algorithm is convergent.*

**Proof:** Similarly, the convergence of the proposed SCA-based alternating algorithm is guaranteed by the following two facts. First, the objective value in Problem (P2) is non-increasing over iterations. More specifically, during each iteration, the variable  $g$  satisfies  $g \geq 0$ , which means  $f_{o\Phi}^{(q)} \geq f_{ow}^{(q)}$ . Furthermore, if  $\mathbf{w}^{(q+1)}$  is the optimal solution to Problem (P8) during the  $(q+1)^{\text{th}}$  iteration, we obtain  $f_{ow}^{(q+1)} \geq f_{o\Phi}^{(q)}$ . Therefore, we have  $f_{ow}^{(q+1)} \geq f_{o\Phi}^{(q)} \geq f_{ow}^{(q)}$ , indicating that  $P_t^{(q+1)} \leq P_t^{(q)}$ . Hence, the transmit power at the BS  $P_t$  is non-increasing over the iterations. Second, the optimal value is bounded from below due to the SNR constraints for Problem (P2). Therefore, the proposed SCA-based alternating algorithm is convergent.  $\square$

### C. Complexity analysis

The procedure of the SDR-based algorithm is shown in Algorithm 1, which shows that steps 4 and 9 take a major part of the complexity because steps 4 and 9 solve Problems (P3) and (P7), respectively. The complexities of solving Problems (P3) and (P7) include the complexities of 1) solving the SDP problem by utilizing the CVX tool and 2) Gaussian randomization process. CVX first transforms Problems (P3) and (P7) into the standard SDP problems and then utilizes an interior point method (IPM) to obtain the solution. There are  $(K+M^2)$  variances in the standard SDP form of Problem (P3), and the IPM requires  $\mathcal{O}(\sqrt{K+M^2})$  iterations and costs  $\mathcal{O}\left((K+M^2)^3\right)$  arithmetic operations in each iteration to obtain a solution [18]. Furthermore, the eigenvalue decomposition of  $\mathbf{X}$  of size  $M \times M$  takes a major part of the computational complexity in the Gaussian randomization process, which requires  $\mathcal{O}(M^3)$  arithmetic operations [48]. Then, the complexity of solving Problem (P3) is  $\mathcal{O}\left((K+M^2)^{3.5} + M^3\right)$ . Similarly, the complexity of solving Problem (P7) is  $\mathcal{O}\left((2K+(N+1)^2)^{3.5} + (N+1)^3\right)$ . Finally, the complexity of the SDR-based algorithm is  $\mathcal{O}\left(L_{\text{SDR}}\left((K+M^2)^{3.5} + M^3 + (2K+(N+1)^2)^{3.5} + (N+1)^3\right)\right)$  where  $L_{\text{SDR}}$  denotes the number of iterations of the SDR-based algorithm.

The procedure of the SCA-based algorithm is shown in Algorithm 2, and steps 4 and 9 take a major part of complexity because steps 4 and 9 solve Problems (P8) and (P9), respectively. Similar to Problem (P3), the complexity of solving Problem (P9) is  $\mathcal{O}\left((K+(N+1)^2)^{3.5} + (N+1)^3\right)$  for one iteration. Furthermore, the SCA method obtains a solution to Problem (P8) by solving  $(\text{P8}')$  iteratively, and we use  $I_{\text{SCA}}^{\text{P8}}$  to denote the number of iterations. Similar to Problem (P3), we compute the complexity of the standard form of  $(\text{P8}')$  which is a second-order cone programming (SOCP). Let  $q$  be the number of Linear Matrix Inequality (LMI) constraints,  $m$  be the number of SOC constraints,  $k_j$  denote the size of the  $j^{\text{th}}$  LMI or SOC constraint, and  $n$  represent the total number of variables of the standard form of  $(\text{P8}')$ . Then, the complexity of solving the standard  $(\text{P8}')$  is  $\sqrt{\alpha}C$  where  $\sqrt{\alpha} = \sqrt{\sum_{j=1}^q k_j + 2m}$  is the iteration complexity and  $C = n \sum_{j=1}^q k_j^3 + n^2 \sum_{j=1}^q k_j^2 + n \sum_{j=1}^m k_j^2 + n^3$  is the per-iteration computation cost [49]. Note that,  $\{x_i, y_i\}$  in Problem  $(\text{P8}')$  can be expressed as expressions in CVX and thus we do not regard them as variances. For the standard form of Problem  $(\text{P8}')$ , the total number of variables is  $n = M+1$  and there are  $K$  LMIs of size 1 and one SOC of size  $M+1$  in constraints. Therefore, the total complexity of the SCA-based method is  $\mathcal{O}\left(I_{\text{SCA}}\left(I_{\text{SCA}}^{\text{P8}}\sqrt{K+2}(M+1)^3 + (K+(N+1)^2)^{3.5} + (N+1)^3\right)\right)$ , where  $I_{\text{SCA}}$  is the number of alternating optimization iterations for the SCA-based method.

We can see that the highest complexity orders of the SCA-based algorithm and the SDR-based algorithm are  $(M^3, N^7)$  and  $(M^7, N^7)$ . So, the complexity of the SDR-based algorithm is much higher than that of the SCA-based algorithm for the massive MIMO scenarios. Furthermore, the simulation results in Section VI will show that the SCA-based method outperforms the SDR-based method. Note that, all computations are executed at the BS with strong data computing capability and do not increase the amount of calculation on the MEs and RIS sides.

## V. LOWER BOUNDS FOR THE AVERAGE TRANSMIT POWER

In this section, we first derive an analytical lower bound and then a tighter semi-analytical lower bound. In particular, we show how the lower bounds depend on the number of RIS units  $N$ , the number of MEs  $K$ , and the number of antennas  $M$ . The following two case studies are considered: 1)  $K = 1$  and  $M > 1$ , and 2)  $K > 1$  and  $M > 1$ . In addition, when discussing the setup  $K = 1$ , we omit the subscript  $i$  (ME index) of  $\beta_{b,i}$  and  $\beta_{r,i}$  for ease of presentation. For benchmarking purposes, we also derive analytical lower bounds for the transmit power without the RIS and with random phase shifts at the RIS.

We consider the independent and identically distributed (i.i.d) Rayleigh fading channel model for the RIS- $i^{\text{th}}$  ME and BS- $i^{\text{th}}$  ME links<sup>2</sup>, i.e.  $\mathbf{h}_{r,i} \sim \mathcal{CN}(0, \beta_{r,i}^2 \mathbf{I})$  and  $\mathbf{h}_{b,i} \sim \mathcal{CN}(0, \beta_{b,i}^2 \mathbf{I})$  where  $\beta_{r,i}^2$  and  $\beta_{b,i}^2$  account for the path loss, and a full-rank LoS channel model for the BS-RIS link. Let  $(x_{\text{BS}}, y_{\text{BS}}, z_{\text{BS}})$  and  $(x_{\text{RIS}}, y_{\text{RIS}}, z_{\text{RIS}})$  be the coordinates of the BS and the RIS, respectively. Let  $\mathbf{H}_{b,r,m,n}$  denote the channel response between the  $m^{\text{th}}$  antenna of the BS and the  $n^{\text{th}}$  element at the RIS. Then, the full-rank LoS channel between the BS and the RIS is given by [9]

$$\begin{aligned} \mathbf{H}_{b,r,m,n} = & \beta_{b,r} \exp \left( j \frac{2\pi}{\lambda} d_{\text{BS}} ((m-1) \sin \phi_{LoS_1(n)} \sin \theta_{LoS_1(n)}) \right) \\ & \times \exp \left( j \frac{2\pi}{\lambda} d_{\text{RIS}} ((n-1) \sin \phi_{LoS_2(n)} \sin \theta_{LoS_2(n)}) \right), \quad m = 1, \dots, M, \quad n = 1, \dots, N, \end{aligned} \quad (16)$$

where  $\lambda$  is the wavelength,  $d_{\text{BS}}$  and  $d_{\text{RIS}}$  are the inter-antenna distances at the BS and the RIS, respectively.  $\phi_{LoS_1}(n)$  and  $\phi_{LoS_2}(n)$  denote the azimuth angles at the BS and the RIS, respectively,  $\theta_{LoS_1}(n)$  and  $\theta_{LoS_2}(n)$  denote the elevation angle of departure at the BS and the elevation angle

<sup>2</sup>The BS and the RIS are fixed in position while MEs may be in motion. Commonly, the direct line of BS-ME or RIS-ME is obstructed by buildings or something else. In such case, the amplitude fluctuations of the received signal follow Rayleigh distribution [50], thereby adopting the Rayleigh fading channels for the BS-ME and RIS-ME links. In particular, when analyzing transmission technologies, the typical way is to consider the tractable i.i.d Rayleigh fading channel model [51]. In fact, the i.i.d Rayleigh fading channel is reasonable in isotropic scatterer environment when the RIS and the BS are in uniform linear array (ULA) with  $\lambda/2$ -spacing, as in [51]–[53].

of arrival at the RIS, respectively, and  $\beta_{b,r}$  accounts for the path loss of the BS-RIS channel.  $\phi_{LoS_1}(n)$  and  $\theta_{LoS_1}(n)$  are generated uniformly between 0 to  $2\pi$  and 0 to  $\pi$ , respectively, and satisfy  $\phi_{LoS_2}(n) = \pi + \phi_{LoS_1}(n)$ ,  $\theta_{LoS_2}(n) = \pi - \theta_{LoS_1}(n)$  [9]. We can see from (16) that, the path losses between any antenna at the BS and any element at the RIS are the same (i.e.,  $\beta_{b,r}^2$  in (16)). This is because the distance between the BS and the RIS is relatively large compared to the size of the RIS [39], such as the far-field regime [54].

#### A. Lower bounds for the average transmit power in RIS aided systems

Since the BS-MEs and RIS-MEs channels are random variables, we focus on analyzing the lower bound for the average transmit power in RIS aided systems<sup>3</sup>. We first present an analytical lower bound. To get a tighter lower bound, we further derive a semi-analytical lower bound.

1) *Analytical lower bound :*

**Case 1):**  $K = 1$  and  $M > 1$

To obtain the minimum transmit power, the QoS constraint inequality in Problem (P1) needs to be fulfilled with equality, i.e.,  $P_t |\mathbf{h}_1^H(\Phi)\bar{\mathbf{w}}|^2 = \gamma\sigma^2$ . In fact, the optimized  $\Phi$  and  $\mathbf{w}$  maximize the value of  $|\mathbf{h}_1^H(\Phi)\bar{\mathbf{w}}|^2$  since  $\gamma\sigma^2$  is constant, thus obtaining the minimum transmit power  $P_t$ .

The BS-MEs and RIS-MEs channels are random variables. For each realization of these random variables, we can obtain the optimized  $\Phi$  and  $\mathbf{w}$  by utilizing our proposed optimization methods, and can obtain the maximum value of  $|\mathbf{h}_1^H(\Phi)\bar{\mathbf{w}}|^2$ . Then, we can obtain the average maximum value of  $|\mathbf{h}_1^H(\Phi)\bar{\mathbf{w}}|^2$ , and thus the average transmit power can be formulated as

$$\bar{P}_t = \frac{\sigma^2\gamma}{\mathbb{E}(\max(|\mathbf{h}_1^H(\Phi)\bar{\mathbf{w}}|^2))}. \quad (17)$$

As for  $|\mathbf{h}_1^H(\Phi)\bar{\mathbf{w}}|$ , we have [7]

$$|\mathbf{h}_1^H(\Phi)\bar{\mathbf{w}}| = |\mathbf{h}_{r,1}^H\Phi\mathbf{H}_{b,r}\bar{\mathbf{w}} + \mathbf{h}_{b,1}^H\bar{\mathbf{w}}| \stackrel{(a)}{\leq} |\mathbf{h}_{r,1}^H\Phi\mathbf{H}_{b,r}\bar{\mathbf{w}}| + |\mathbf{h}_{b,1}^H\bar{\mathbf{w}}|. \quad (18)$$

Based on the triangle inequality, inequality (a) takes the equality sign if and only if  $\arg(\mathbf{h}_{r,1}^H\Phi\mathbf{H}_{b,r}\bar{\mathbf{w}}) = \arg(\mathbf{h}_{b,1}^H\bar{\mathbf{w}}) = \varphi_0$  [7]. Define  $A := |\mathbf{h}_{r,1}^H\Phi\mathbf{H}_{b,r}\bar{\mathbf{w}}|$ ,  $B := |\mathbf{h}_{b,1}^H\bar{\mathbf{w}}|$ . Then, based on (18), we have [1]

$$\mathbb{E}(\max(|\mathbf{h}_1^H(\Phi)\bar{\mathbf{w}}|^2)) = \mathbb{E}((A+B)^2) = \mathbb{E}(A^2) + 2\mathbb{E}(AB) + \mathbb{E}(B^2). \quad (19)$$

<sup>3</sup>The proposed optimization algorithms are not for some particular channels. The proposed method of deriving the lower bounds for the RIS-aided system is based on the LoS channel and i.i.d Rayleigh fading channel, which requires the first and second central moments of the amplitudes of considered channels. The spatially correlated Rician fading channel couples the amplitudes of the LoS channel and spatially correlated Rayleigh fading channel [55]. Based on the triangle inequality, the spatially correlated Rician fading channel can be decoupled into the LoS channel and spatially correlated Rayleigh fading channel in terms of amplitude. Furthermore, the spatially correlated Rayleigh fading channel can be represented by a linear combination of multiple i.i.d Rayleigh fading channels [56]. Thus, based on the triangle inequality, the spatially correlated Rayleigh fading channel can be decoupled into the sum of multiple i.i.d Rayleigh fading channels in terms of amplitude. Therefore, the method of deriving lower bounds in our paper can be easily extended to the spatially correlated Rician fading channel.



Thus, to derive the lower bound for the average transmit power  $\overline{P}_t$ , we need to compute the maximum value of  $\mathbb{E}(\max(|\mathbf{h}_1^H(\Phi)\overline{\mathbf{w}}|^2))$  with respect to  $\Phi$  and  $\overline{\mathbf{w}}$  [1], denoted by  $Q_1$ , i.e.,

$$Q_1 = \max_{\Phi, \overline{\mathbf{w}}} (\mathbb{E}(A^2) + 2\mathbb{E}(AB) + \mathbb{E}(B^2)). \quad (20)$$

Next, we discuss how to compute  $\mathbb{E}(A^2)$ ,  $\mathbb{E}(AB)$  and  $\mathbb{E}(B^2)$ , thereby deriving  $Q_1$ .

Define  $C_n := \sum_{m=1}^M \mathbf{H}_{b,r,m,n} \overline{w}_m$  ( $n = 1, \dots, N$ ). Then, we have

$$\begin{aligned} |C_n|^2 &= \left| \sum_{m=1}^M H_{b,r,m,n} \overline{w}_m \right|^2 = |H_{b,r,1,n} \overline{w}_1 + \dots + H_{b,r,M,n} \overline{w}_M|^2 \\ &\stackrel{(a)}{\leq} \sum_{m=1}^M |H_{b,r,m,n} \overline{w}_m|^2 + 2 \sum_{t=1}^M \sum_{k=t+1}^M |H_{b,r,t,n} \overline{w}_t| |H_{b,r,k,n} \overline{w}_k| \\ &= |H_{b,r,1,n}|^2 + \left( 2 |H_{b,r,1,n}|^2 \sum_{t=1}^M \sum_{k=t+1}^M |\overline{w}_t| |\overline{w}_k| \right) \stackrel{(b)}{\leq} |H_{b,r,1,n}|^2 M \stackrel{(c)}{=} M \beta_{b,r}^2, \end{aligned} \quad (21)$$

where step (a) follows from the fact that  $\left| \sum_{m=1}^M H_{b,r,m,n} \overline{w}_m \right| \leq \sum_{m=1}^M |H_{b,r,m,n} \overline{w}_m|$ , step (b) follows from the fact that the term  $(|\overline{w}_k| |\overline{w}_t|)$  takes the maximum value if  $|\overline{w}_k| = |\overline{w}_t|$ , which yields  $|\overline{w}_1|^2 = \dots = |\overline{w}_M|^2 = \frac{1}{M}$  because  $\sum_{m=1}^M |\overline{w}_m|^2 = 1$ , and step (c) follows from the fact that the elements in  $\mathbf{H}_{b,r}$  have the same amplitude since the distance between the BS and the RIS is relatively large compared to the size of the RIS.

As for  $\mathbb{E}(A^2)$ , we have

$$\mathbb{E}(A) \stackrel{(a)}{=} \mathbb{E} \left( \sum_{n=1}^N |h_{r,1,n}^H| \left| \sum_{m=1}^M H_{b,r,m,n} \overline{w}_m \right| \right) \stackrel{(b)}{=} \mathbb{E}(|h_{r,1,1}^H|) \left( \sum_{n=1}^N |C_n| \right) \stackrel{(c)}{\leq} \frac{\sqrt{\pi M N} \beta_{b,r} \beta_r}{2}, \quad (22a)$$

$$\begin{aligned} \mathbb{E}(A^2) &= \mathbb{E} \left( \left( \sum_{n=1}^N |h_{r,i,n}^H| |C_n| \right)^2 \right) \\ &= \mathbb{E} \left( \sum_{n=1}^N (|h_{r,1,n}^H|^2 |C_n|^2) + 2 \sum_{n=1}^N \sum_{i=n+1}^N |h_{r,1,n}^H| |C_n| |h_{r,1,i}^H| |C_i| \right) \\ &= \mathbb{E} (|h_{r,1,1}^H|^2) \sum_{n=1}^N (|C_n|^2) + 2 \mathbb{E}^2 (|h_{r,1,1}^H|) \sum_{n=1}^N \sum_{i=n+1}^N |C_n| |C_i| \\ &\stackrel{(d)}{\leq} \frac{\pi N^2 \beta_{b,r}^2 \beta_r^2 M}{4} + \frac{N \beta_r^2 \beta_{b,r}^2 M}{2} \left( 2 - \frac{\pi}{2} \right), \end{aligned} \quad (22b)$$

where step (a) follows from the fact that  $\arg(\mathbf{h}_{r,1}^H \Phi \mathbf{H}_{b,r} \overline{\mathbf{w}}) = \varphi_0$ , step (b) follows from the fact that  $\mathbf{h}_{r,1} \sim \mathcal{CN}(0, \beta_{r,1}^2 \mathbf{I})$ , step (c) is derived based on the Cauchy–Schwartz inequality, and steps (c) and (d) follow from the fact that  $|C_n|^2 \leq M \beta_{b,r}^2$  ( $n = 1, \dots, N$ ) as shown in (21) and that  $|h_{r,1,1}^H|$  has a Rayleigh distribution with variance  $\frac{\beta_r^2}{2} (2 - \frac{\pi}{2})$ .

As for  $\mathbb{E}(B^2)$ , we have [1]

$$\mathbb{E}(B) = \mathbb{E} \left( \left| \sum_{m=1}^M h_{b,m} H \overline{w}_m \right| \right) \stackrel{(a)}{\leq} \mathbb{E} \left( \sum_{m=1}^M |h_{b,m} H \overline{w}_m| \right) = \mathbb{E}(|h_{b,1}^H|) \sum_{m=1}^M |\overline{w}_m|, \quad (23a)$$

$$\mathbb{E}^2(B) = \mathbb{E}^2(|h_{b,1}^H|) \left( \sum_{m=1}^M |\overline{w}_m| \right)^2 \stackrel{(b)}{\leq} (M|\overline{w}_1|)^2 \frac{\beta_b^2 \pi}{4} = \frac{\pi \beta_b^2 M}{4}, \quad (23b)$$

$$\begin{aligned} \mathbb{E}(B^2) &\leq \mathbb{E} \left( \left( \sum_{m=1}^M |h_{b,m} H \overline{w}_m| \right)^2 \right) \\ &= \mathbb{E} \left( \sum_{m=1}^M (|h_{b,m}^H|^2 |\overline{w}_m|^2) + 2 \sum_{m=1}^M \sum_{i=m+1}^M |h_{b,m}^H| |\overline{w}_m| |h_{b,i}^H| |\overline{w}_i| \right) \\ &= \mathbb{E} (|h_{b,1}^H|^2) \sum_{m=1}^M (|\overline{w}_m|^2) + 2\mathbb{E}^2|h_{b,1}^H| \sum_{m=1}^M \sum_{i=M+1}^M \|\overline{w}_m\| \|\overline{w}_i\| \stackrel{(b)}{\leq} \frac{\pi \beta_b^2 M}{4} + \frac{\beta_b^2}{2} (2 - \frac{\pi}{2}), \end{aligned} \quad (23c)$$

where step (a) follows from the fact that  $\left| \sum_{m=1}^M h_{b,m} H \overline{w}_m \right| \leq \sum_{m=1}^M |h_{b,m} H \overline{w}_m|$ , steps (b) and (c) follow from the fact that  $|h_{b,1}^H|$  has a Rayleigh distribution with mean  $\frac{\beta_b \sqrt{\pi}}{2}$  and variance  $\frac{\beta_b^2}{2} (2 - \frac{\pi}{2})$ , step (b) follows from the fact that the term  $(|\overline{w}_1| + |\overline{w}_2| + \dots + |\overline{w}_M|)^2$  takes the maximum value if  $|\overline{w}_1| = |\overline{w}_2| = \dots = |\overline{w}_M|$  because  $\sum_{m=1}^M |\overline{w}_m|^2 = 1$ .

As for  $\mathbb{E}(AB)$ , given  $\overline{w}$ , variables  $A$  and  $B$  are independent of each other. Hence, we have

$$\mathbb{E}(AB) = \sqrt{\mathbb{E}^2(A)\mathbb{E}^2(B)} \leq \frac{N\pi\beta_r\beta_{b,r}\beta_b M}{4}. \quad (24)$$

When  $|\overline{w}_1| = \dots = |\overline{w}_M|$  and  $|C_1| = \dots = |C_N|$ , (22b), (23c) and (24) hold with the equality sign. Then, we can formulate  $Q_1$  as follows

$$\begin{aligned} Q_1 &= \max_{\Phi, \overline{w}} (\mathbb{E}(A^2) + 2\mathbb{E}(AB) + \mathbb{E}(B^2)) \\ &= \frac{\pi N^2 \beta_{b,r}^2 \beta_r^2 M}{4} + \frac{N \beta_r^2 \beta_{b,r}^2 M}{2} (2 - \frac{\pi}{2}) + \frac{N \pi \beta_r \beta_{b,r} \beta_b M}{2} + \frac{\beta_b^2}{2} (2 - \frac{\pi}{2}) + \frac{\pi \beta_b^2 M}{4}. \end{aligned} \quad (25)$$

Based on (17), a lower bound for the average transmit power at the BS is given by

$$P_{K=1, M>1}^L = \frac{\sigma^2 \gamma}{Q_1} = \frac{\sigma^2 \gamma}{\frac{\pi N^2 \beta_b^2 \beta_r^2 M}{4} + \frac{N \beta_r^2 \beta_{b,r}^2 M}{2} (2 - \frac{\pi}{2}) + \frac{N \pi \beta_r \beta_{b,r} \beta_b M}{2} + \frac{\beta_b^2}{2} (2 - \frac{\pi}{2}) + \frac{\pi \beta_b^2 M}{4}}, \quad (26)$$

where the superscript “ $L$ ” is used to denote “lower bound”. (26) confirms that the average transmit power of an RIS scales with  $1/N^2$  [57].

**Case 2):  $K > 1$  and  $M > 1$**

Based on Problem (P1) and (10), the average transmit power  $\overline{P}_t$  is [1]

$$\overline{P}_t = \frac{\gamma\sigma^2}{\min(\mathbb{E}(\max(|\mathbf{h}_1^H(\Phi)\overline{\mathbf{w}}|^2)), \dots, \mathbb{E}(\max(|\mathbf{h}_K^H(\Phi)\overline{\mathbf{w}}|^2)))}. \quad (27)$$

By using the inequality  $\min(\mathbb{E}(\max(|\mathbf{h}_1^H(\Phi)\overline{\mathbf{w}}|^2)), \dots, \mathbb{E}(\max(|\mathbf{h}_i^H(\Phi)\overline{\mathbf{w}}|^2)), \dots, \mathbb{E}(\max(|\mathbf{h}_K^H(\Phi)\overline{\mathbf{w}}|^2))) \leq \min(Q_1, \dots, Q_i, \dots, Q_K)$ , a lower bound for the average transmit power at the BS is [1]

$$P_{K>1, M>1}^L = \frac{\gamma\sigma^2}{\min(Q_1, \dots, Q_i, \dots, Q_K)}, \quad (28)$$

where  $Q_i$  is the maximum value of  $\mathbb{E}(\max(|h_i^H(\Phi)\overline{\mathbf{w}}|^2))$  with respect to  $\Phi$  and  $\overline{\mathbf{w}}$ . (22)–(25) allow us to compute  $Q_1$ . A similar approach is used to compute other values of  $Q_i$  ( $i = 1, \dots, K$ ).

2) *Semi-analytical lower bound:*

**Case 1):**  $K = 1$  and  $M > 1$

The maximum value of  $\mathbb{E}(\max(|\mathbf{h}_1^H(\Phi)\overline{\mathbf{w}}|^2))$  with respect to  $\Phi$  and  $\overline{\mathbf{w}}$  is

$Q_1 = \max_{\Phi, \overline{\mathbf{w}}}(\mathbb{E}(A^2) + 2\mathbb{E}(AB) + \mathbb{E}(B^2))$  in (20). In the following, we compute each term of  $Q_1$ .

Define  $C_n := \sum_{m=1}^M \mathbf{H}_{b,r,m,n} \overline{w}_m$ . Then, we have

$$\begin{aligned} |C_n| &= \sqrt{\left| \sum_{m=1}^M H_{b,r,m,n} \overline{w}_m \right|^2} = \sqrt{\left| \sum_{m=1}^M |H_{b,r,m,n}| |\overline{w}_m| \exp(j(\varphi_{H_{b,r,m,n}} + \varphi_{w_m})) \right|^2} \\ &= \sqrt{|H_{b,r,1,1}|^2 \left| \sum_{m=1}^M |\overline{w}_m| \exp(j(\varphi_{H_{b,r,m,n}} + \varphi_{w_m})) \right|^2} \stackrel{(a)}{=} \sqrt{|H_{b,r,1,1}|^2 \left| \sum_{m=1}^M |\overline{w}_m| \exp(j(\varphi_{m,n})) \right|^2} \\ &= \sqrt{|H_{b,r,1,1}|^2 \left| \sum_{m=1}^M |\overline{w}_m| (\cos(\varphi_{m,n}) + j\sin(\varphi_{m,n})) \right|^2} \\ &= \sqrt{|H_{b,r,1,1}|^2 \left( \sum_{m=1}^M |\overline{w}_m|^2 (\cos^2(\varphi_{m,n}) + \sin^2(\varphi_{m,n})) + 2 \sum_{k=1}^M \sum_{t=k+1}^M (|\overline{w}_k| |\overline{w}_t| (\cos(\varphi_{k,n} - \varphi_{t,n}))) \right)} \\ &\stackrel{(b)}{\leq} \sqrt{(\beta_{b,r})^2 \left( 1 + \frac{2}{M} \sum_{k=1}^M \sum_{t=k+1}^M ((\cos(\varphi_{k,n} - \varphi_{t,n}))) \right)} \\ &\stackrel{(c)}{=} \sqrt{(\beta_{b,r})^2 \left( 1 + \frac{2}{M} \sum_{k=1}^M \sum_{t=k+1}^M ((\cos(\text{const}_{k,t,n} + \varphi_{w_k - w_t})) \right)} \stackrel{(d)}{=} \sqrt{(\beta_{b,r})^2 \left( 1 + \frac{2}{M} \sum_{k=1}^M \sum_{t=k+1}^M f_c(w_k, w_t) \right)}, \end{aligned} \quad (29)$$

where step (a) is derived by defining  $\varphi_{m,n} := \varphi_{H_{b,r,m,n}} + \varphi_{w_m}$  where  $\varphi_c$  denotes the angle of a complex number  $c$ , step (b) follows from the fact that the term  $(|\overline{w}_k| |\overline{w}_t|)$  takes the maximum

value if  $|\overline{w_k}| = |\overline{w_t}|$ , which implies  $|\overline{w_1}|^2 = \dots = |\overline{w_M}|^2 = \frac{1}{M}$  because  $\sum_{m=1}^M |\overline{w_m}|^2 = 1$ , step (c) is obtained by using  $\varphi_{k,n} - \varphi_{t,n} = \varphi_{H_{b,r,k,n}} - \varphi_{H_{b,r,t,n}} + \varphi_{w_k} - \varphi_{w_t} = \text{const}_{k,t,n} + \varphi_{w_k} - \varphi_{w_t}$  and defining  $\varphi_{w_k} - \varphi_{w_t} := \varphi_{w_k - w_t}$ , and step (d) is derived by defining  $f_c(w_k, w_t) := \cos(\text{const}_{k,n} + \varphi_{w_k - w_t})$ .

As for  $\mathbb{E}(A^2)$ , we have

$$\mathbb{E}(A) \stackrel{(a)}{=} \mathbb{E} \left( \sum_{n=1}^N |h_{r,1,n}^H| \left| \sum_{m=1}^M H_{b,r,m,n} \overline{w_m} \right| \right) \stackrel{(b)}{=} \frac{\beta_r \sqrt{\pi}}{2} \left( \sum_{n=1}^N |C_n| \right), \quad (30a)$$

$$\begin{aligned} \mathbb{E}(A^2) &= \mathbb{E} \left( \left( \sum_{n=1}^N |h_{r,i,n}^H| |C_n| \right)^2 \right) \\ &= \mathbb{E} \left( \sum_{n=1}^N (|h_{r,i,n}^H|^2 |C_n|^2) + 2 \sum_{n=1}^N \sum_{i=n+1}^N |h_{r,i,n}^H| |C_n| |h_{r,1,i}^H| |C_i| \right) \\ &= \mathbb{E} (|h_{r,1,1}^H|^2) \sum_{n=1}^N (|C_n|^2) + 2 \mathbb{E}^2 (|h_{r,1,1}^H|) \sum_{n=1}^N \sum_{i=n+1}^N |C_n| |C_i| \\ &\stackrel{(d)}{=} \sum_{n=1}^N (\beta_r^2 (|C_n|^2)) + 2 \sum_{n=1}^N \sum_{i=n+1}^N \frac{(\beta_r)^2 \pi}{4} |C_n| |C_i|, \end{aligned} \quad (30b)$$

where step (a) follows from  $\arg(\mathbf{h}_{r,1}^H \Phi \mathbf{H}_{b,r} \overline{\mathbf{w}}) = \varphi_0$ , and steps (b) and (c) follow from the fact that  $|h_{r,1,1}^H|$  has a Rayleigh distribution with mean  $\beta_r \sqrt{\pi}/2$  and variance  $\beta_r^2/2(2 - \pi/2)$ .

Similarly, as for  $\mathbb{E}(B^2)$ , we have

$$\begin{aligned} \mathbb{E}(B^2) &= \mathbb{E} \left( \left| \sum_{m=1}^M h_{b,1,m} \overline{w_m} \right|^2 \right) = \mathbb{E} \left( \left| \sum_{m=1}^M |h_{b,1,m}| |\overline{w_m}| \exp(j(\varphi_{h_{b,1,m}} + \varphi_{w_m})) \right|^2 \right) \\ &= \mathbb{E} \left( \left| \sum_{m=1}^M |h_{b,1,m}| |\overline{w_m}| \cos(\varphi_{h_{b,1,m}} + \varphi_{w_m}) + j \sum_{m=1}^M |h_{b,1,m}| |\overline{w_m}| \sin(\varphi_{h_{b,1,m}} + \varphi_{w_m}) \right|^2 \right) \\ &= \mathbb{E} \left( \left( \sum_{m=1}^M |h_{b,1,m}| |\overline{w_m}| \cos(\varphi_{h_{b,1,m}} + \varphi_{w_m}) \right)^2 + \left( \sum_{m=1}^M |h_{b,1,m}| |\overline{w_m}| \sin(\varphi_{h_{b,1,m}} + \varphi_{w_m}) \right)^2 \right) \\ &= \mathbb{E} \left( \sum_{m=1}^M |h_{b,1,m}|^2 |\overline{w_m}|^2 (\cos^2(\varphi_{h_{b,1,m}} + \varphi_{w_m}) + \sin^2(\varphi_{h_{b,1,m}} + \varphi_{w_m})) \right) \\ &\quad + \mathbb{E} \left( 2 \sum_{k=1}^M \sum_{t=k+1}^M (|h_{b,1,k}| |\overline{w_k}| |h_{b,1,t}| |\overline{w_t}| (\cos(\varphi_{h_{b,1,k}} - \varphi_{h_{b,1,t}} + \varphi_{w_k} - \varphi_{w_t}))) \right) \\ &\stackrel{(a)}{=} \left( \frac{(\beta_b)^2 \pi}{4} + \frac{\beta_b^2}{2} (2 - \frac{\pi}{2}) \right) \left( \sum_{m=1}^M |\overline{w_m}|^2 \right) + \frac{(\beta_b)^2 \pi}{4} \left( 2 \sum_{k=1}^M \sum_{t=k+1}^M (|\overline{w_k}| |\overline{w_t}| (\cos(\varphi_{h_{b,1,k}} - \varphi_{h_{b,1,t}} + \varphi_{w_k} - \varphi_{w_t}))) \right) \end{aligned}$$

$$\begin{aligned}
&\stackrel{(b)}{\leq} \frac{(\beta_b)^2 \pi}{4} \left( 1 + \frac{2}{M} \sum_{k=1}^M \sum_{t=k+1}^M ((\cos(\varphi_{h,k,t} + \varphi_{w_k - w_t})) \right) + \frac{\beta_b^2}{2} (2 - \frac{\pi}{2}) \\
&\stackrel{(c)}{=} \frac{(\beta_b)^2 \pi}{4} \left( 1 + \frac{2}{M} \sum_{k=1}^M \sum_{t=k+1}^M f_b(w_k, w_t) \right) + \frac{\beta_b^2}{2} (2 - \frac{\pi}{2}),
\end{aligned} \tag{31}$$

where step (a) is derived by the fact that  $|h_{b,1,1}^H|$  has a Rayleigh distribution with mean  $\frac{\beta_b \sqrt{\pi}}{2}$  and defining  $\varphi_{h_{b,1,k}} - \varphi_{h_{b,1,t}} + \varphi_{w_k} - \varphi_{w_t} := \varphi_{h,k,t} + \varphi_{w_k - w_t}$ , step (b) follows from the fact that the term  $(|\overline{w}_k| |\overline{w}_t|)$  takes the maximum value if  $|\overline{w}_k| = |\overline{w}_t|$  which implies  $|\overline{w}_1|^2 = \dots = |\overline{w}_M|^2 = \frac{1}{M}$  because  $\sum_{m=1}^M |\overline{w}_m|^2 = 1$ , and step (c) is derived by defining  $f_b(w_k, w_t) := \cos(\varphi_{h,k,t} + \varphi_{w_k - w_t})$ .

As for  $\mathbb{E}(AB)$ , since  $\mathbb{E}^2(B) \leq \frac{\pi \beta_b^2 M}{4}$  based on (23), we have

$$\mathbb{E}(AB) = \sqrt{\mathbb{E}^2(A) \mathbb{E}^2(B)} \leq \left( \sum_{n=1}^N \sqrt{(\beta_{b,r})^2 \left( 1 + \frac{2}{M} \sum_{k=1}^M \sum_{t=k+1}^M f_c(w_k, w_t) \right)} \right) \frac{\pi \beta_r \beta_b \sqrt{M}}{4}. \tag{32}$$

Based on (29)-(32), we evince that the upper bounds of  $\mathbb{E}(A^2)$ ,  $\mathbb{E}(B^2)$  and  $\mathbb{E}(AB)$  are related to variables  $w_1, \dots, w_M$ . Therefore, the upper bound of  $(\mathbb{E}(A^2) + \mathbb{E}(B^2) + 2\mathbb{E}(AB))$  is related to variables  $w_1, \dots, w_M$ , which is denoted by  $f_1(w_1, \dots, w_M)$  and can be written as follows

$$\begin{aligned}
&\mathbb{E}(A^2) + \mathbb{E}(B^2) + 2\mathbb{E}(AB) \leq f_1(w_1, \dots, w_M) \\
&= \left( \sum_{n=1}^N \sqrt{(\beta_{b,r})^2 \left( 1 + \frac{2}{M} \sum_{k=1}^M \sum_{t=k+1}^M f_c(w_k, w_t) \right)} \right)^2 \frac{\beta_r^2 \pi}{4} \\
&+ \frac{\beta_r^2}{2} (2 - \frac{\pi}{2}) \times \left( \sum_{n=1}^N (\beta_{b,r})^2 \left( 1 + \frac{2}{M} \sum_{k=1}^M \sum_{t=k+1}^M f_c(w_k, w_t) \right) \right) + \frac{(\beta_b)^2 \pi}{4} \left( 1 + \frac{2}{M} \sum_{k=1}^M \sum_{t=k+1}^M f_b(w_k, w_t) \right) \\
&+ \frac{\beta_b^2}{2} (2 - \frac{\pi}{2}) + 2 \left( \sum_{n=1}^N \sqrt{(\beta_{b,r})^2 \left( 1 + \frac{2}{M} \sum_{k=1}^M \sum_{t=k+1}^M f_c(w_k, w_t) \right)} \right) \frac{\pi \beta_r \beta_b \sqrt{M}}{4}.
\end{aligned} \tag{33}$$

Thus,  $Q_1$  is the maximum value of  $f_1(w_1, \dots, w_M)$ , which can be formulated as follows

$$Q_1 = \max_{w_1, \dots, w_M} f_1(w_1, \dots, w_M). \tag{34}$$

Based on (17), a lower bound for the average transmit power at the BS is given by

$$P_{K=1, M>1}^L = \frac{\sigma^2 \gamma}{Q_1} = \frac{\sigma^2 \gamma}{\max_{w_1, \dots, w_M} f_1(w_1, \dots, w_M)}. \tag{35}$$

Since the value of  $f_1(w_1, \dots, w_M)$  depends on  $f_c(w_k, w_t) := ((\cos(\text{const}_{k,n} + \varphi_{w_k - w_t}))$  and  $f_b(w_k, w_t) := \cos(\varphi_{w_k - w_t})$  based on (33),  $f_1$  depends on the phase difference of two antennas at the BS (i.e.,  $\varphi_{w_k - w_t}$ ) which ranges from 0 to  $2\pi$ . Therefore, we utilize a brute-force method

to find phase differences that maximize the value of  $f_1$ . This means that a lower bound for the average transmit power for such case is in a semi-analytical form.

**Case 2):**  $K > 1$  and  $M > 1$

By using the inequality  $\min(\mathbb{E}(\max(|\mathbf{h}_1^H(\Phi)\bar{\mathbf{w}}|^2)), \dots, \mathbb{E}(\max(|\mathbf{h}_i^H(\Phi)\bar{\mathbf{w}}|^2)), \dots, \mathbb{E}(\max(|\mathbf{h}_K^H(\Phi)\bar{\mathbf{w}}|^2))) \leq \min(Q_1, \dots, Q_i, \dots, Q_K)$  and (34), a lower bound for the average transmit power at the BS is given by

$$P_{K>1, M>1}^L = \frac{\gamma\sigma^2}{\min(Q_1, Q_2, \dots, Q_K)} = \frac{\gamma\sigma^2}{\max_{w_1, \dots, w_M} \min(f_1, f_2, \dots, f_K)}. \quad (36)$$

(29)–(34) allow us to compute  $f_1$ . A similar approach can be used to compute other values of  $f_i$  ( $i = 1, \dots, K$ ). Based on (34), we can derive that (36) depends on the phase difference of two antennas at the BS which ranges from 0 to  $2\pi$ . We can also utilize a brute-force method to find phase differences that maximize the value of  $\min(f_1, f_2, \dots, f_K)$ .

**Remark 1** (*Relation between the analytical lower bound and the semi-analytical lower bound*).

When all of the  $\cos$  terms in step (c) of (31) and step (b) of (33) equal the maximum value 1, terms  $|C_n|$  and  $\mathbb{E}(B^2)$  in the semi-analytical lower bound are equal to those in the analytical lower bound, respectively. Then, it is easy to derive that the semi-analytical lower bound is equal to the analytical lower bound. In turn, if all of the  $\cos$  terms in step (c) of (29) and step (b) of (31) equal the maximum value 1, we have  $\varphi_{h,k,t} + \varphi_{w_k} - \varphi_{w_t} = 0$  and  $\text{const}_{k,n} + \varphi_{w_k} - \varphi_{w_t} = 0$ , where  $\varphi_c$  denotes the angle of a complex number  $c$ . We derive that  $\text{const}_{k,t,n} = \varphi_{h,k,t}$  i.e.,  $\varphi_{H_{b,r,k,n}} - \varphi_{H_{b,r,t,n}} = \varphi_{h_{b,1,k}} - \varphi_{h_{b,1,t}}$  where  $\mathbf{H}_{b,r,k(or t),n}$  denotes the channel response between the ( $k(or t)$ )<sup>th</sup> antenna of the BS and the  $n^{\text{th}}$  element at the RIS. However, based on the full-rank LoS channel model in (16) and the uncorrelated Rayleigh fading channel between the BS and each ME, this does not hold. Hence, it is impossible to ensure that all of the  $\cos$  terms in step (c) of (29) and step (b) of (31) equal the maximum value 1, which indicates that the semi-analytical bound can never equal the analytical bound. Compared to the analytical lower bound, the semi-analytical lower bound is closer to the simulation results. However, the analytical lower bound can intuitively show advantages of the RIS.

*B. Analytical lower bound for the average transmit power with random phase shifts at the RIS*

**Case 1):**  $K = 1$  and  $M > 1$

Similar to RIS aided systems, the maximum value of  $\mathbb{E}(\max(|\mathbf{h}_1^H(\Phi)\bar{\mathbf{w}}|^2))$  with respect to  $\bar{\mathbf{w}}$  is  $Q_1 = \max_{\bar{\mathbf{w}}}(\mathbb{E}(A^2) + 2\mathbb{E}(AB) + \mathbb{E}(B^2))$ . We discuss how to compute each term of  $Q_1$ .

Recalling  $A = |\mathbf{h}_{r,1}^H \Phi \mathbf{H}_{b,r} \bar{\mathbf{w}}| = \left| \sum_{n=1}^N h_{r,1,n}^H e^{j\theta_1^{(n)}} \sum_{m=1}^M H_{b,r,m,n} \bar{w}_m \right| = \left| \sum_{n=1}^N h_{r,1,n}^H e^{j\theta_1^{(n)}} C_n \right|$ , we obtain that  $\sum_{n=1}^N h_{r,1,n}^H e^{j\theta_1^{(n)}} C_n$  has a circularly-symmetric complex Gaussian distribution with mean 0 and variance  $(|C_1|^2 + \dots + |C_N|^2) \text{Var}(h_{r,1,1}) = (|C_1|^2 + \dots + |C_N|^2) \beta_r^2$ . Then,  $A$  follows a Rayleigh distribution with mean  $\frac{\sqrt{|C_1|^2 + \dots + |C_N|^2} \beta_r \sqrt{\pi}}{2}$  and variance  $\frac{(|C_1|^2 + \dots + |C_N|^2) \beta_r^2}{2} (2 - \frac{\pi}{2})$ .

Hence, we have

$$\begin{aligned} \mathbb{E}(A^2) &= \mathbb{E}^2(A) + \text{Var}(A) = \left( \frac{\sqrt{|C_1|^2 + \dots + |C_N|^2} \beta_r \sqrt{\pi}}{2} \right)^2 + \frac{(|C_1|^2 + \dots + |C_N|^2) \beta_r^2}{2} (2 - \frac{\pi}{2}) \\ &= (|C_1|^2 + \dots + |C_N|^2) \beta_r^2 \left( \frac{\pi}{4} + \frac{1}{2} (2 - \frac{\pi}{2}) \right) \stackrel{(a)}{\leq} NM \beta_{b,r}^2 \beta_r^2, \end{aligned} \quad (37)$$

where step (a) derives from (21), i.e.,  $|C_n|^2 \leq M \beta_{b,r}^2$  ( $n = 1, \dots, N$ ).

$\mathbb{E}(B^2)$  is the same as we derived in (23), i.e.,  $\mathbb{E}(B^2) \leq \frac{\pi \beta_b^2 M}{4} + \frac{\beta_b^2}{2} (2 - \frac{\pi}{2})$ .

As for  $\mathbb{E}(AB)$ , since  $\mathbb{E}^2(B) \leq \frac{\pi \beta_b^2 M}{4}$  based on (23), we have

$$\mathbb{E}(AB) = \sqrt{\mathbb{E}^2(A) \mathbb{E}^2(B)} \leq \frac{\sqrt{N} \pi \beta_r \beta_{b,r} \beta_b M}{4}. \quad (38)$$

When  $|\bar{w}_1| = \dots = |\bar{w}_M|$  and  $|C_1| = \dots = |C_N|$ , (37), (23), and (38) hold with the equality sign. Then,  $Q_1$  can be formulated as follows

$$Q_1 = \max_{\bar{\mathbf{w}}} (\mathbb{E}(A^2) + 2\mathbb{E}(AB) + \mathbb{E}(B^2)) = NM \beta_{b,r}^2 \beta_r^2 + \frac{\sqrt{N} \pi \beta_r \beta_{b,r} \beta_b M}{2} + \frac{\pi \beta_b^2 M}{4} + \frac{\beta_b^2}{2} (2 - \frac{\pi}{2}). \quad (39)$$

Based on (17), a lower bound for the average transmit power at the BS is given by

$$P_{K=1, M>1}^L = \frac{\sigma^2 \gamma}{Q_1} = \frac{\sigma^2 \gamma}{NM \beta_{b,r}^2 \beta_r^2 + \frac{\sqrt{N} \pi \beta_r \beta_{b,r} \beta_b M}{2} + \frac{\pi \beta_b^2 M}{4} + \frac{\beta_b^2}{2} (2 - \frac{\pi}{2})}. \quad (40)$$

(40) confirms that the average transmit power with random phase shifts at the RIS nearly scales with  $1/N$ .

**Case 2):**  $K > 1$  and  $M > 1$

The lower bound expression for such case is the same as (28), where the value of  $Q_i$  ( $i = 1, \dots, K$ ) can be computed by utilizing the same method used for obtaining  $Q_1$  in (39).

### C. Analytical lower bound for the average transmit power without the RIS

**Case 1):**  $K = 1$  and  $M > 1$

For such case, there exist only the direct channels between the BS and MEs. Hence, we have  $Q_1 = \max_{\bar{\mathbf{w}}} \mathbb{E}(B^2)$ . Based on (23), we have  $Q_1 = \max_{\bar{\mathbf{w}}} \mathbb{E}(B^2) = \frac{\pi \beta_b^2 M}{4} + \frac{\beta_b^2}{2} (2 - \frac{\pi}{2})$ . Then, a lower bound for the average transmit power at the BS is

$$P_{K=1, M>1}^L = \frac{\sigma^2 \gamma}{Q_1} = \frac{\sigma^2 \gamma}{\frac{\pi \beta_b^2 M}{4} + \frac{\beta_b^2}{2} (2 - \frac{\pi}{2})}. \quad (41)$$

**Case 2):  $K > 1$  and  $M > 1$**

The lower bound expression for such case is the same as (28), where the value of  $Q_i$  ( $i = 1, \dots, K$ ) can be computed by utilizing the same method used for obtaining  $Q_1$  in (23).

**Remark 2** (*What happens if the CSI is in error*). For Problem (P1), the SNR constraint (i.e., the QoS requirement) is represented by the CSI. If the estimated CSI is in error, the CSI can be represented by the sum of the estimated CSI and the estimation error. However, we can only obtain the estimated CSI and cannot know the estimation error in practice. Therefore, to formulate the problem under imperfect CSI estimation, the key is to tackle the CSI estimation error in SNR and ensure the QoS requirement at the same time. Then, the optimization algorithms can be designed to solve the optimization problem under imperfect CSI estimation. Authors in [20] have dealt with how to tackle such problem, but they only considered the imperfect RIS-ME CSI estimation and assumed perfect BS-RIS and BS-ME CSI estimation. The constraints under imperfect RIS-ME, BS-RIS, and RIS-ME CSI estimations are more complex than the case in [20], which are left for our future work. The performance of the proposed optimization algorithms and the derived lower bounds in this paper can be viewed as benchmarks.

**Remark 3** (*Differences between our paper, [58] and the single-ME optimization problem in [7]*). Both our paper, [58], and [7] aim to minimize the transmit power at the BS. The main differences between our paper and [58] [7] are discussed as follows.

Both [58] and our paper aim to minimize the transmit power at the BS over broadcasting signals 1) but for different RIS-aided systems. More specifically, [58] was for symbiotic radio system to support passive Internet of Things (IoT), where the RIS is not only to reflect signals from the BS but also needs to transmit data to other MEs. In contrast, our paper is to support active IoT where the RIS is only used to reflect signals from the BS. 2) Authors in [58] decoupled the original problem into two subproblems and utilized the SDR method to solve them, which is similar to our proposed SDR-based method but our approach is more general. The reason is that it is the action of the RIS transmitting data to other MEs in [58] that makes the constraints for decoding the transmitted signal at the BS in [58] be a particular case of the constraints in our problem. 3) To reduce the computational complexity and improve the performance of the SDR-based optimization algorithm, we also propose an SCA-based alternating optimization algorithm. 4) Though authors in [58] solved the problem of discrete phase shifts, the discrete



phase shifts were obtained by just quantifying the derived continuous phase shifts. Therefore, the key is to design the optimization algorithms for the continuous phase shifts problem in [58]. Our paper considers the continuous phase shifts. We can obtain the discrete phase shifts by quantifying the derived continuous phase shifts or other optimization algorithms, which are left for our future work. The performance of the proposed optimization algorithms with continuous phase shifts in this paper can be viewed as a benchmark. Furthermore, we derive two lower bounds of the average transmit power at the BS in our paper further to analyze the effectiveness of our proposed optimization algorithms. In contrast, authors in [58] did not present the lower bounds to analyze the effectiveness of their proposed optimization algorithm. The method of deriving the lower bounds can be utilized for the problem in [58]. The reason is that the lower bounds for the problem in [58] and our problem are determined by the constraints, and the constraints in [58] are the special case of the constraints in our paper.

For [7] and our paper, the RIS is only used to reflect signals from the BS to MEs. 1) From the perspective of the problem formulation, the only difference is considering the SNR constraints at multiple MEs in our paper instead of the SNR constraint at single ME in the single-ME optimization problem of [7]. However, this difference induces significant differences in problem-solving between our paper and [7]. Specifically, for the single-ME optimization problem in [7], the maximum-ratio transmission is the optimal transmit beamforming solution to this single-ME optimization problem when given phase shifts, and the phase shifts at the RIS can be tuned to achieve the maximum combined channel gains for a signal ME at the same time. Based on these observations, authors in [7] proposed two approaches to solve the single-ME optimization problem, which cannot be utilized to solve our problem for multiple MEs. The reason is that, for multiple MEs, our problem is NP-hard when given phase shifts [18], and the phase shifts cannot be tuned to achieve the maximum combined channel gains for all MEs at the same time because all MEs with different channels share the same phase shifts. The single-ME optimization problem in [7] is a particular case of our problem (i.e.,  $K = 1$ ), and thus our proposed optimization algorithms can solve the single-ME optimization problem in [7] as well, which means that our methods are more general. 2) Furthermore, we derive analytical and semi-analytical lower bounds for the average transmit power at the BS for the general case (i.e., multiple MEs and a multi-antenna BS) to analyze the effectiveness of the proposed optimization algorithms. Authors in [7] just presented the analytical result of scaling law of the transmit power at the BS with the number of elements at the RIS based on a particular case (i.e., a single ME and

a single-antenna BS), aiming to obtain an insight into the advantage of the RIS. 3) In addition, we present the detailed procedure of how to derive lower bounds based on the LoS BS-to-RIS channel and i.i.d Rayleigh fading BS-to-ME and RIS-to-ME channels and briefly show how to extend our derived lower bounds to the generalized spatially correlated Rician fading channels. The analytical result in [7] is only based on i.i.d Rayleigh fading BS-RIS and RIS-ME channel and ignoring the BS-ME channel. Thus, the method of deriving lower bounds in our paper is more general.

## VI. SIMULATION RESULTS

In this section, we utilize numerical results to validate the proposed optimization algorithms and the derived lower bounds. We assume that a BS with a uniform linear array of antennas is located at  $(0, 0, 0)$ , and an RIS with a uniform linear array of RIS units is located at  $(0, 50, 0)$ . The inter-antenna and inter-unit separation at the BS and the RIS are a half of the wavelength. The purpose of deploying the RIS is to improve the signal strength. To illustrate this benefit, we assume that the MEs are uniformly located within the half-circle centered at the RIS with radius 3 m as shown in Fig. 2, which are the cell-edge MEs.

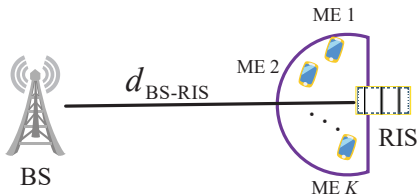


Fig. 2: The location of the RIS, BS and MEs in the simulation.

The channel models for the BS-RIS, BS-MEs and RIS-MEs are the same as those we described in Section V. The path loss between  $a$  and  $b$  is  $C_0(d_{a,b}/D_0)^{-\alpha}$ , where  $C_0 = 1$  m,  $D_0 = -30$  dB,  $d_{a,b}$  denotes the distance between  $a$  and  $b$ , and  $\alpha$  is the path loss exponent. We set  $\sigma^2 = -30$  dBm, and  $\varepsilon = 10^{-4}$ . For the BS-RIS, RIS-MEs, and BS-MEs, we set  $\alpha$  to be 2, 2.8, and 3.5, respectively. As the baselines, we employ the conventional power control (i.e., MMSE and ZF based beamforming, termed “Without-RIS-MMSE” and “Without-RIS-ZF”, respectively, in the figures), power control with random phase shifts at the RIS (termed “Random-RIS” in the figures), and a two-stage algorithm proposed in [7]. The MMSE-based beamforming is obtained by solving Problem (P2) and setting  $\Phi = \mathbf{0}$ , and the ZF-based beamforming is obtained according to  $\text{trace} \left( \text{diag} \left( (\sigma_1)^2 \gamma_1, \dots, (\sigma_K)^2 \gamma_K \right) \times \left( \mathbf{H}_b^H \mathbf{H}_b \right)^{-1} \right)$  [7]. In addition, the

terms “alternating optimization algorithm based on SDR”, “alternating optimization algorithm based on SCA”, “analytical lower bound for the average transmit power in RIS aided systems”, and “semi-analytical lower bound for the average transmit power in RIS aided systems” are abbreviated as “With-RIS-SDR”, “With-RIS-SCA”, “With-RIS-LB1” and “With-RIS-LB2” in the figures, respectively. Terms “analytical lower bound for the average transmit power with random phase shifts at the RIS” and “analytical lower bound for the transmit power without the RIS” are abbreviated as “Random-RIS-LB” and “Without-RIS-LB” in the figures, respectively.

Note that, for the single-ME case, since the result obtained by the MMSE-based beamforming is the same as that obtained by the ZF-based beamforming, we use the term “Without-RIS” to denote the conventional power control scheme. Furthermore, the semi-analytical lower bound for the average transmit power depends on the phase difference between any two antennas. We utilize the brute-force method to obtain the semi-analytical lower bound with 500 quantization levels when  $M$  is small. To resolve the search explosion when  $M$  is sufficiently large, we utilize a random search method [59] to obtain the semi-analytical lower bound.

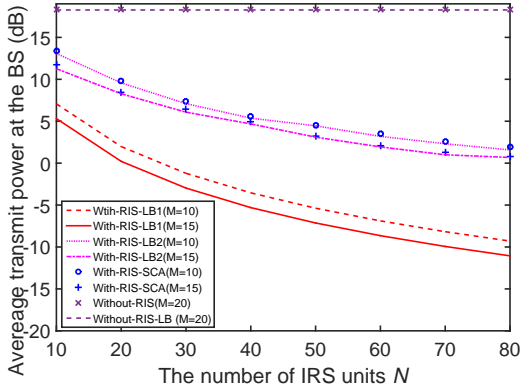


Fig. 3: Average transmit power at the BS versus the number of RIS units  $N$  for single-ME case.

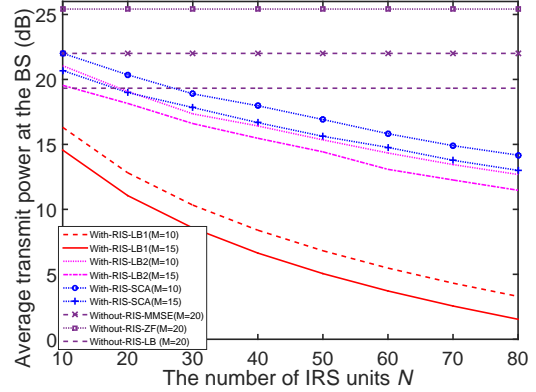


Fig. 4: Average transmit power at the BS versus the number of RIS units  $N$  for multi-MEs case.

Figs. 3 and 4 show how average transmit power at the BS changes with the number of RIS units  $N$  under  $\gamma = 1$  dB for  $K = 1$  and  $K = 5$ , respectively. We can observe that, in RIS aided systems, with the increase of the number of RIS units  $N$  and the number of antennas at the BS, the average transmit power decreases significantly. Furthermore, the simulation results are closer to semi-analytical lower bound, compared to the analytical lower bound which intuitively show the transmit power scales with  $1/N^2$  in the context of RIS communication systems. The reason is given in Remark 1. We can also observe that with the increase of the number of MEs, the performance gap between RIS aided systems and the system without the RIS widens up

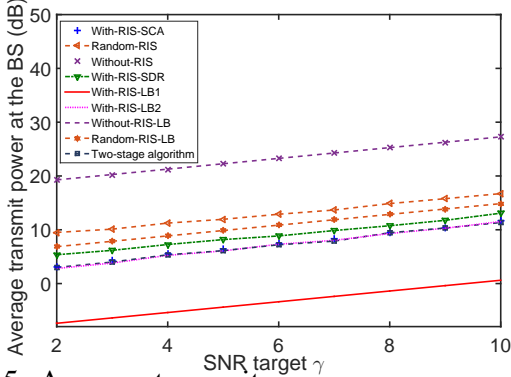


Fig. 5: Average transmit power versus SNR target  $\gamma$  for single-ME case.

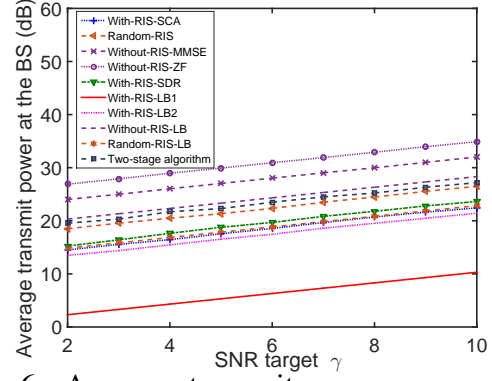


Fig. 6: Average transmit power versus SNR target  $\gamma$  for multi-MEs case.

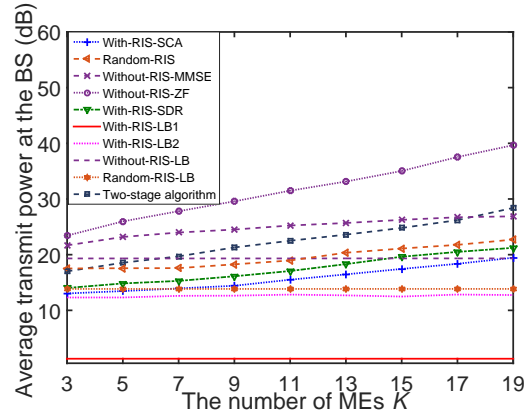


Fig. 7: Average transmit power versus the number of MEs  $K$ .

gradually, which coincides with the trend obtained from the lower bounds. Interestingly, the average transmit power at the BS in RIS aided systems is much lower than the average transmit power without the RIS, even when the number of antennas at the BS in RIS aided systems (i.e.,  $M = 10, 15$ ) is less than that without the RIS (i.e.,  $M = 20$ ). This means that RIS aided systems with low-power consumption elements can increase the energy efficiency.

Figs. 5 and 6 show how average transmit power at the BS changes with the SNR target  $\gamma$  ranging from 2 to 10 under  $M = 20, N = 70$  for  $K = 1$  and  $K = 5$ , respectively. We can observe from the results that the average transmit power at the BS increases almost linearly with the increase in the SNR target for single-ME and multi-MEs cases. We can also see that, when  $\gamma$  ranges from 2 to 10, the semi-analytical lower bound is closer to the simulation results, compared to the analytical lower bound. In addition, among these baselines, the two-stage algorithm with the lower complexity of  $\mathcal{O}((K + M^2)^{3.5} + ((N + 1)^2)^{3.5})$  achieves the same performance gain as our proposed alternating optimization algorithm based on SCA and coincides with the semi-analytical lower bound for the single-ME case, while the transmit power at the BS of our proposed

alternating optimization algorithms is significantly lower than that of the two-stage algorithm for the multi-MEs case. The reason is that, the performance of the two-stage algorithm close to optimal. However, for the multi-MEs case, since the phase shifts at the RIS are same for all MEs with different channel gain, the two-stage algorithm cannot maximize the combined channel power gain of different MEs simultaneously [7].

Fig. 7 shows how the average transmit power at the BS changes with the number of MEs for  $M = 20$ ,  $\gamma = 1$  dB, and  $N = 70$ . The results show that, with the increase of the number of MEs, the average transmit power increases, and is dramatically lower than the baselines. This means that RIS aided systems can increase the energy efficiency.

## VII. CONCLUSION

In this paper, we have proposed algorithms for power control problem at the BS with QoS constraints in RIS aided wireless systems. Specifically, we have utilized alternating optimization algorithms to jointly optimize the transmit beamforming at the BS and the phase shifts at the RIS. Furthermore, we have derived lower bounds for the average transmit power. Simulation results have showed that the average transmit power at the BS is close to the lower bound, and is significantly lower than that of communication systems without the RIS.

## REFERENCES

- [1] H. Han, J. Zhao, D. Niyato, M. D. Renzo, and Q.-V. Pham, "Intelligent reflecting surface aided network: power control for physical-layer broadcasting," in *2020 IEEE International Conference on Communications (ICC), Dublin, Ireland, Jun. 7-11, 2020*.
- [2] C. Huang, A. Zappone, G. C. Alexandropoulos, M. Debbah, and C. Yuen, "Reconfigurable intelligent surfaces for energy efficiency in wireless communication," *IEEE Transactions on Wireless Communications*, vol. 18, no. 8, pp. 4157–4170, Aug. 2019.
- [3] M. Di Renzo, A. Zappone, M. Debbah, M.-S. Alouini, C. Yuen, J. de Rosny, and S. Tretyakov, "Smart radio environments empowered by reconfigurable intelligent surfaces: How it works, state of research, and the road ahead," *IEEE Journal on Selected Areas in Communications*, vol. 38, no. 11, pp. 2450–2525, 2020.
- [4] C. Huang, G. C. Alexandropoulos, C. Yuen, and M. Debbah, "Indoor signal focusing with deep learning designed reconfigurable intelligent surfaces," in *2019 IEEE 20th International Workshop on Signal Processing Advances in Wireless Communications (SPAWC), 2019*, pp. 1–5.
- [5] C. Huang, G. C. Alexandropoulos, A. Zappone, M. Debbah, and C. Yuen, "Energy efficient multi-user MISO communication using low resolution large intelligent surfaces," in *2018 IEEE Globecom Workshops, GC Wkshps, Abu Dhabi, United Arab Emirates, Dec. 9-13, 2018*, pp. 1–6.
- [6] J. Ye, S. Guo, and M. S. Alouini, "Joint reflecting and precoding designs for SER minimization in reconfigurable intelligent surfaces assisted MIMO systems," *IEEE Transactions on Wireless Communications*, vol. 19, no. 8, pp. 5561–5574, 2020.

- [7] Q. Wu and R. Zhang, "Intelligent reflecting surface enhanced wireless network via joint active and passive beamforming," *IEEE Transactions on Wireless Communications*, vol. 18, no. 11, pp. 5394–5409, Nov. 2019.
- [8] Q. Wu and R. Zhang, "Beamforming optimization for intelligent reflecting surface with discrete phase shifts," in *2019 IEEE International Conference on Acoustics, Speech and Signal Processing (ICASSP), Brighton, United Kingdom, May 12-17, 2019*, pp. 7830–7833.
- [9] Q. Nadeem, A. Kammoun, A. Chaaban, M. Debbah, and M. Alouini, "Asymptotic max-min sinr analysis of reconfigurable intelligent surface assisted MISO systems," *IEEE Transactions on Wireless Communications*, pp. 1–1, 2020.
- [10] E. Basar, M. Di Renzo, J. De Rosny, M. Debbah, M. Alouini, and R. Zhang, "Wireless communications through reconfigurable intelligent surfaces," *IEEE Access*, vol. 7, pp. 116 753–116 773, 2019.
- [11] C. Huang, S. Hu, G. C. Alexandropoulos, A. Zappone, C. Yuen, R. Zhang, M. D. Renzo, and M. Debbah, "Holographic mimo surfaces for 6G wireless networks: Opportunities, challenges, and trends," *IEEE Wireless Communications*, vol. 27, no. 5, pp. 118–125, 2020.
- [12] M. Di Renzo and J. Song, "Reflection probability in wireless networks with metasurface-coated environmental objects: an approach based on random spatial processes," *EURASIP Journal on Wireless Communication and Networking*, vol. 2019, no. 1, p. 99, Apr. 2019.
- [13] N. Rajatheva, I. Atzeni, and e. a. Emil Bjornson, "White paper on broadband connectivity in 6G," *arXiv preprint arXiv:2004.14247*, 2020.
- [14] Q. Wu, S. Zhang, B. Zheng, C. You, and R. Zhang, "Intelligent reflecting surface-aided wireless communications: A tutorial," *IEEE Transactions on Communications*, vol. 69, no. 5, pp. 3313–3351, 2021.
- [15] Q. Wu and R. Zhang, "Intelligent reflecting surface enhanced wireless network: Joint active and passive beamforming design," in *2018 IEEE Global Communications Conference (GLOBECOM)*, 2018, pp. 1–6.
- [16] Q.-U.-A. Nadeem, H. Alwazani, A. Kammoun, A. Chaaban, M. Debbah, and M.-S. Alouini, "Intelligent reflecting surface-assisted multi-user MISO communication: Channel estimation and beamforming design," *IEEE Open Journal of the Communications Society*, vol. 1, pp. 661–680, 2020.
- [17] 3GPP, "Radio resource control (RRC) protocol specification (Release 16)," Sep. 2020.
- [18] N. D. Sidiropoulos, T. N. Davidson, and Z.-Q. Luo, "Transmit beamforming for physical-layer multicasting," *IEEE Transactions on Signal Processing*, vol. 54, no. 6, pp. 2239–2250, Jun. 2006.
- [19] Q. Wu and R. Zhang, "Beamforming optimization for wireless network aided by intelligent reflecting surface with discrete phase shifts," *IEEE Transactions on Communications*, vol. 68, no. 3, pp. 1838–1851, Mar. 2020.
- [20] G. Zhou, C. Pan, H. Ren, K. Wang, M. D. Renzo, and A. Nallanathan, "Robust beamforming design for intelligent reflecting surface aided MISO communication systems," *IEEE Wireless Communications Letters*, vol. 9, no. 10, pp. 1658–1662, 2020.
- [21] Z. Chu, W. Hao, P. Xiao, and J. Shi, "Intelligent reflecting surface aided multi-antenna secure transmission," *IEEE Wireless Communications Letters*, vol. 9, no. 1, pp. 108–112, Jan. 2020.
- [22] B. Feng, Y. Wu, and M. Zheng, "Secure transmission strategy for intelligent reflecting surface enhanced wireless system," in *2019 IEEE International Conference on Wireless Communications and Signal Processing (WCSP), Xi'an, China, Oct. 23-25, 2019*, pp. 1–6.
- [23] Y. Li, M. Jiang, Q. Zhang, and J. Qin, "Joint beamforming design in multi-cluster MISO NOMA intelligent reflecting surface-aided downlink communication networks," *arXiv preprint arXiv:1909.06972*, 2019.
- [24] M. Fu, Y. Zhou, and Y. Shi, "Intelligent reflecting surface for downlink non-orthogonal multiple access networks," in *2019 IEEE Globecom Workshops (GC Wkshps), Hawaii, USA, Dec.9-13, 2019*, pp. 1–6.
- [25] J. Zhao, "Optimizations with intelligent reflecting surfaces (IRSs) in 6G wireless networks: Power control, quality of

- service, max-min fair beamforming for unicast, broadcast, and multicast with multi-antenna mobile users and multiple irss,” *arXiv preprint arXiv:1908.03965*, 2019.
- [26] Q. Wu and R. Zhang, “Joint active and passive beamforming optimization for intelligent reflecting surface assisted SWIPT under QoS constraints,” *IEEE Journal on Selected Areas in Communications*, vol. 38, no. 8, pp. 1735–1748, 2020.
- [27] G. Zhou, C. Pan, H. Ren, K. Wang, and A. Nallanathan, “Intelligent reflecting surface aided multigroup multicast MISO communication systems,” *IEEE Transactions on Signal Processing*, pp. 1–1, 2020.
- [28] L. Du, J. Ma, Q. Liang, and Y. Tang, “Multiple antenna multicast transmission assisted by reconfigurable intelligent surfaces,” *arXiv preprint arXiv:1912.07960*, 2019.
- [29] N. Sidiropoulos, T. Davidson, and Z.-Q. Luo, “Transmit beamforming for physical-layer multicasting,” *IEEE Transactions on Signal Processing*, vol. 54, no. 6, pp. 2239–2251, Jun. 2006.
- [30] E. Karipidis, N. D. Sidiropoulos, and Z.-Q. Luo, “Quality of service and max-min fair transmit beamforming to multiple cochannel multicast groups,” *IEEE Transactions on Signal Processing*, vol. 56, no. 3, pp. 1268–1279, Mar. 2008.
- [31] J. Choi, “Minimum power multicast beamforming with superposition coding for multiresolution broadcast and application to NOMA systems,” *IEEE Transactions on Communications*, vol. 63, no. 3, pp. 791–800, Mar. 2015.
- [32] H. Guo, Y.-C. Liang, J. Chen, and E. G. Larsson, “Weighted sum-rate optimization for intelligent reflecting surface enhanced wireless networks,” *arXiv preprint arXiv:1905.07920*.
- [33] T. S. Rappaport, G. R. MacCartney, M. K. Samimi, and S. Sun, “Wideband millimeter-wave propagation measurements and channel models for future wireless communication system design,” *IEEE Transactions on Communications*, vol. 63, no. 9, pp. 3029–3056, Sep. 2015.
- [34] M. Di Renzo, K. Ntontin, J. Song, F. H. Danufane, X. Qian, F. Lazarakis, J. De Rosny, D.-T. Phan-Huy, O. Simeone, R. Zhang, M. Debbah, G. Lerosey, M. Fink, S. Tretyakov, and S. Shamai, “Reconfigurable intelligent surfaces vs. relaying: Differences, similarities, and performance comparison,” *IEEE Open Journal of the Communications Society*, vol. 1, pp. 798–807, 2020.
- [35] Q. Wu and R. Zhang, “Towards smart and reconfigurable environment: Intelligent reflecting surface aided wireless network,” *IEEE Communications Magazine*, vol. 58, no. 1, pp. 106–112, Jan. 2020.
- [36] X. Tan, Z. Sun, D. Koutsonikolas, and J. M. Jornet, “Enabling indoor mobile millimeter-wave networks based on smart reflect-arrays,” in *in 2018 IEEE Conference on Computer Communications (INFOCOM), Honolulu, HI, USA, Apr. 16-19, 2018*, pp. 270–278.
- [37] W. Tang, M. Z. Chen, X. Chen, J. Y. Dai, Y. Han, M. Di Renzo, Y. Zeng, S. Jin, Q. Cheng, and T. J. Cui, “Wireless communications with reconfigurable intelligent surface: Path loss modeling and experimental measurement,” *IEEE Transactions on Wireless Communications*, vol. 20, no. 1, pp. 421–439, 2021.
- [38] W. Tang, J. Y. Dai, M. Z. Chen, K.-K. Wong, X. Li, X. Zhao, S. Jin, Q. Cheng, and T. J. Cui, “MIMO transmission through reconfigurable intelligent surface: System design, analysis, and implementation,” *IEEE Journal on Selected Areas in Communications*, vol. 38, no. 11, pp. 2683–2699, 2020.
- [39] L. Dai, B. Wang, M. Wang, X. Yang, J. Tan, S. Bi, S. Xu, F. Yang, Z. Chen, M. D. Renzo, C. Chae, and L. Hanzo, “Reconfigurable intelligent surface-based wireless communications: Antenna design, prototyping, and experimental results,” *IEEE Access*, vol. 8, pp. 45 913–45 923, 2020.
- [40] H. Yang, Z. Xiong, J. Zhao, D. Niyato, Q. Wu, H. V. Poor, and M. Tornatore, “Intelligent reflecting surface assisted anti-jamming communications: A fast reinforcement learning approach,” *IEEE Transactions on Wireless Communications*, pp. 1–1, 2020.
- [41] S. Gong, X. Lu, D. T. Hoang, D. Niyato, L. Shu, D. I. Kim, and Y.-C. Liang, “Towards smart radio environment for

- wireless communications via intelligent reflecting surfaces: A comprehensive survey,” *arXiv preprint arXiv:1912.07794*, 2019.
- [42] S. Abeywickrama, R. Zhang, and C. Yuen, “Intelligent reflecting surface: Practical phase shift model and beamforming optimization,” in *ICC 2020 - 2020 IEEE International Conference on Communications (ICC)*, 2020, pp. 1–6.
- [43] C. Huang, A. Zappone, M. Debbah, and C. Yuen, “Achievable rate maximization by passive intelligent mirrors,” in *2018 IEEE International Conference on Acoustics, Speech and Signal Processing (ICASSP)*, 2018, pp. 3714–3718.
- [44] H. Cramér, *Random Variables and Probability Distributions*. Cambridge University Press, 2004.
- [45] M. Grant and S. Boyd. CVX: MATLAB software for disciplined convex programming. [Online]. Available: <http://cvxr.com/cvx>
- [46] A. M.-C. So, J. Zhang, and Y. Ye, “On approximating complex quadratic optimization problems via semidefinite programming relaxations,” *Mathematical Programming*, vol. 110, no. 1, pp. 93–110, Jul. 2007.
- [47] L. Tran, M. F. Hanif, and M. Juntti, “A conic quadratic programming approach to physical layer multicasting for large-scale antenna arrays,” *IEEE Signal Processing Letters*, vol. 21, no. 1, pp. 114–117, Jan. 2014.
- [48] J. Demmel, I. Dumitriu, and O. Holtz, “Fast linear algebra is stable,” *Numerische Mathematik*, vol. 108, pp. 59–91, 2007.
- [49] K.-Y. Wang, A. M.-C. So, T.-H. Chang, W.-K. Ma, and C.-Y. Chi, “Outage constrained robust transmit optimization for multiuser MISO downlinks: Tractable approximations by conic optimization,” *IEEE Transactions on Signal Processing*, vol. 62, no. 21, pp. 5690–5705, 2014.
- [50] R. H. Clarke, “A statistical theory of mobile-radio reception,” *Bell System Technical Journal* 47, vol. 47, pp. 957–1000, 1968.
- [51] E. Björnson and L. Sanguinetti, “Rayleigh fading modeling and channel hardening for reconfigurable intelligent surfaces,” *IEEE Wireless Communications Letters*, vol. 10, no. 4, pp. 830–834, 2021.
- [52] S. Li, B. Duo, X. Yuan, Y.-C. Liang, and M. Di Renzo, “Reconfigurable intelligent surface assisted uav communication: Joint trajectory design and passive beamforming,” *IEEE Wireless Communications Letters*, vol. 9, no. 5, pp. 716–720, 2020.
- [53] Y. Zhu, G. Zheng, and K.-K. Wong, “Stochastic geometry analysis of large intelligent surface-assisted millimeter wave networks,” *IEEE Journal on Selected Areas in Communications*, vol. 38, no. 8, pp. 1749–1762, 2020.
- [54] M. Di Renzo, F. Habibi Danufane, X. Xi, J. de Rosny, and S. Tretyakov, “Analytical modeling of the path-loss for reconfigurable intelligent surfaces-anomalous mirror or scatterer ?” in *2020 IEEE 21st International Workshop on Signal Processing Advances in Wireless Communications (SPAWC)*, 2020, pp. 1–5.
- [55] Q. Wu and R. Zhang, “Intelligent reflecting surface enhanced wireless network via joint active and passive beamforming,” *IEEE Transactions on Wireless Communications*, vol. 18, no. 11, pp. 5394–5409, Nov. 2019.
- [56] X. Li, X. Yu, T. Sun, J. Guo, and J. Zhang, “Joint scheduling and deep learning-based beamforming for fd-mimo systems over correlated rician fading,” *IEEE Access*, vol. 7, pp. 118 297–118 309, 2019.
- [57] X. Qian, M. Di Renzo, J. Liu, A. Kammoun, and M.-S. Alouini, “Beamforming through reconfigurable intelligent surfaces in single-user MIMO systems: SNR distribution and scaling laws in the presence of channel fading and phase noise,” *IEEE Wireless Communications Letters*, vol. 10, no. 1, pp. 77–81, 2021.
- [58] X. Xu, Y.-C. Liang, G. Yang, and L. Zhao, “Reconfigurable intelligent surface empowered symbiotic radio over broadcasting signals,” in *GLOBECOM 2020 - 2020 IEEE Global Communications Conference*, 2020, pp. 1–6.
- [59] J. Bergstra and Y. Bengio, “Random search for Hyper-Parameter optimization,” *Journal of Machine Learning Research*, vol. 13, pp. 281–305, Feb. 2012.